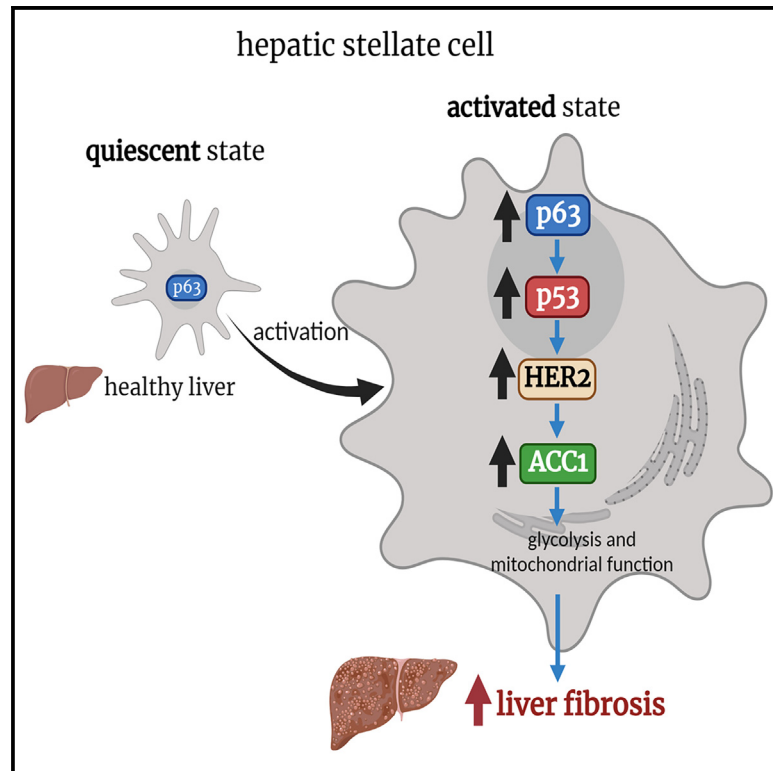**Article**

p63 controls metabolic activation of hepatic stellate cells and fibrosis via an HER2-ACC1 pathway

Graphical abstract

Authors

Marcos F. Fondevila, Eva Novoa,
Maria J. Gonzalez-Rellan, ...,
Javier Crespo, Paula Iruzubieta,
Ruben Nogueiras

Correspondence

marcos.fernandez.fondevila@gmail.com
(M.F.F.),
ruben.nogueiras@usc.es (R.N.)

In brief

Fondevila et al. show that the expression of transcription factor TAp63 is increased in hepatic stellate cells from patients and animals with liver fibrosis. TAp63 induces *de novo* fatty acid synthesis, which activates stellate cells. However, deletion of TAp63 inhibits the activation of these cells and protects against liver fibrosis.

Highlights

- TAp63 is induced in hepatic stellate cells of patients and rodents with fibrosis

- Mice lacking TAp63 in HSCs are protected against liver fibrosis

- TAp63 increases the transcriptional activity of HER2 and ACC1 activity in HSCs

- The genetic inhibition of HER2 or ACC1 blunts TAp63-induced activation of HSCs

CellPress

Article

p63 controls metabolic activation of hepatic stellate cells and fibrosis via an HER2-ACC1 pathway

Marcos F. Fondevila,[1,2,16,*] Eva Novoa,[1,2,16] Maria J. Gonzalez-Rellan,[1,16] Uxia Fernandez,[1,2,16] Violeta Heras,[1] Begoña Porteiro,[1] Tamara Parracho,[1] Valentina Dorta,[1] Cristina Riobello,[3] Natalia da Silva Lima,[1] Samuel Seoane,[1] Maria Garcia-Vence,[4] Maria P. Chantada-Vazquez,[4] Susana B. Bravo,[4] Ana Senra,[1] Magdalena Leiva,[5,6,7] Miguel Marcos,[8] Guadalupe Sabio,[9] Roman Perez-Fernandez,[1] Carlos Dieguez,[1] Vincent Prevot,[10] Markus Schwaninger,[11] Ashwin Woodhoo,[3] Maria L. Martinez-Chantar,[12] Robert Schwabe,[13] Francisco J. Cubero,[5,6,7] Marta Varela-Rey,[3] Javier Crespo,[14] Paula Iruzubieta,[14] and Ruben Nogueiras[1,2,15,17,*]

[1]Department of Physiology, CIMUS, University of Santiago de Compostela, 15782 Santiago de Compostela, Spain
[2]CIBER Fisiopatologia de la Obesidad y Nutrición (CIBERobn), 15782 Santiago de Compostela, Spain
[3]Gene Regulatory Control in Disease Laboratory, Center for Research in Molecular Medicine and Chronic Diseases (CIMUS), Instituto de Investigación Sanitaria de Santiago de Compostela (IDIS), University of Santiago de Compostela, 15782 Santiago de Compostela, Spain
[4]Proteomic Unit, Instituto de Investigación Sanitaria de Santiago de Compostela (IDIS), 15705 Santiago de Compostela, Spain
[5]Department of Immunology, Ophthalmology, & ENT, Complutense University School of Medicine, 28040 Madrid, Spain
[6]Health Research Institute Gregorio Marañón (IiSGM), 28007 Madrid, Spain
[7]CIBER Enfermedades Hepáticas y Digestivas (CIBEREHD), Instituto de Salud Carlos III, 28029 Madrid, Spain
[8]University of Salamanca, Department of Internal Medicine, University Hospital of Salamanca-IBSAL, 37008 Salamanca, Spain
[9]Centro Nacional de Investigaciones Cardiovasculares (CNIC), 28029 Madrid, Spain
[10]University Lille, Inserm, CHU Lille, Laboratory of Development and Plasticity of the Neuroendocrine Brain, Lille Neuroscience & Cognition, European Genomic Institute for Diabetes (EGID), 59000 Lille, France
[11]University of Lübeck, Institute for Experimental and Clinical Pharmacology and Toxicology, 23562 Lübeck, Germany
[12]Liver Disease Lab, Center for Cooperative Research in Biosciences (CIC bioGUNE), Basque Research and Technology Alliance (BRTA), 48160 Derio, Bizkaia, Spain
[13]Department of Medicine, Columbia University, New York, NY 10027, USA
[14]Gastroenterology and Hepatology Department, Marqués de Valdecilla University Hospital, Clinical and Translational Digestive Research Group, IDIVAL, 39008 Santander, Spain
[15]Galicia Agency of Innovation (GAIN), Xunta de Galicia, 15702 Santiago de Compostela, Spain
[16]These authors contributed equally
[17]Lead contact
*Correspondence: marcos.fernandez.fondevila@gmail.com (M.F.F.), ruben.nogueiras@usc.es (R.N.)
https://doi.org/10.1016/j.xcrm.2024.101401

SUMMARY

The p63 protein has pleiotropic functions and, in the liver, participates in the progression of nonalcoholic fatty liver disease (NAFLD). However, its functions in hepatic stellate cells (HSCs) have not yet been explored. TAp63 is induced in HSCs from animal models and patients with liver fibrosis and its levels positively correlate with NAFLD activity score and fibrosis stage. In mice, genetic depletion of TAp63 in HSCs reduces the diet-induced liver fibrosis. *In vitro* silencing of p63 blunts TGF-β1-induced HSCs activation by reducing mitochondrial respiration and glycolysis, as well as decreasing acetyl CoA carboxylase 1 (ACC1). Ectopic expression of TAp63 induces the activation of HSCs and increases the expression and activity of ACC1 by promoting the transcriptional activity of HER2. Genetic inhibition of both HER2 and ACC1 blunt TAp63-induced activation of HSCs. Thus, TAp63 induces HSC activation by stimulating the HER2-ACC1 axis and participates in the development of liver fibrosis.

INTRODUCTION

The p53 family of transcription factors includes not only p53 but also p63 and p73, in which p63 and p73 share high-sequence and structural similarities but can exert different biological effects and act through different mechanisms.[1–3] Despite being recognized mainly for their role in the cell cycle and cancer, there is increasing evidence that this family also influences different metabolic pathways.[4–6]

p63 is expressed as two major isoforms: an TAp63 form that contains an N-terminal transactivation (TA) domain, and an N-terminal truncated (ΔNp63) isoform that lacks this domain.[7,8] p63 acts as a master transcription factor of stem cell pluripotency and is crucial in basal epithelial development, differentiation,
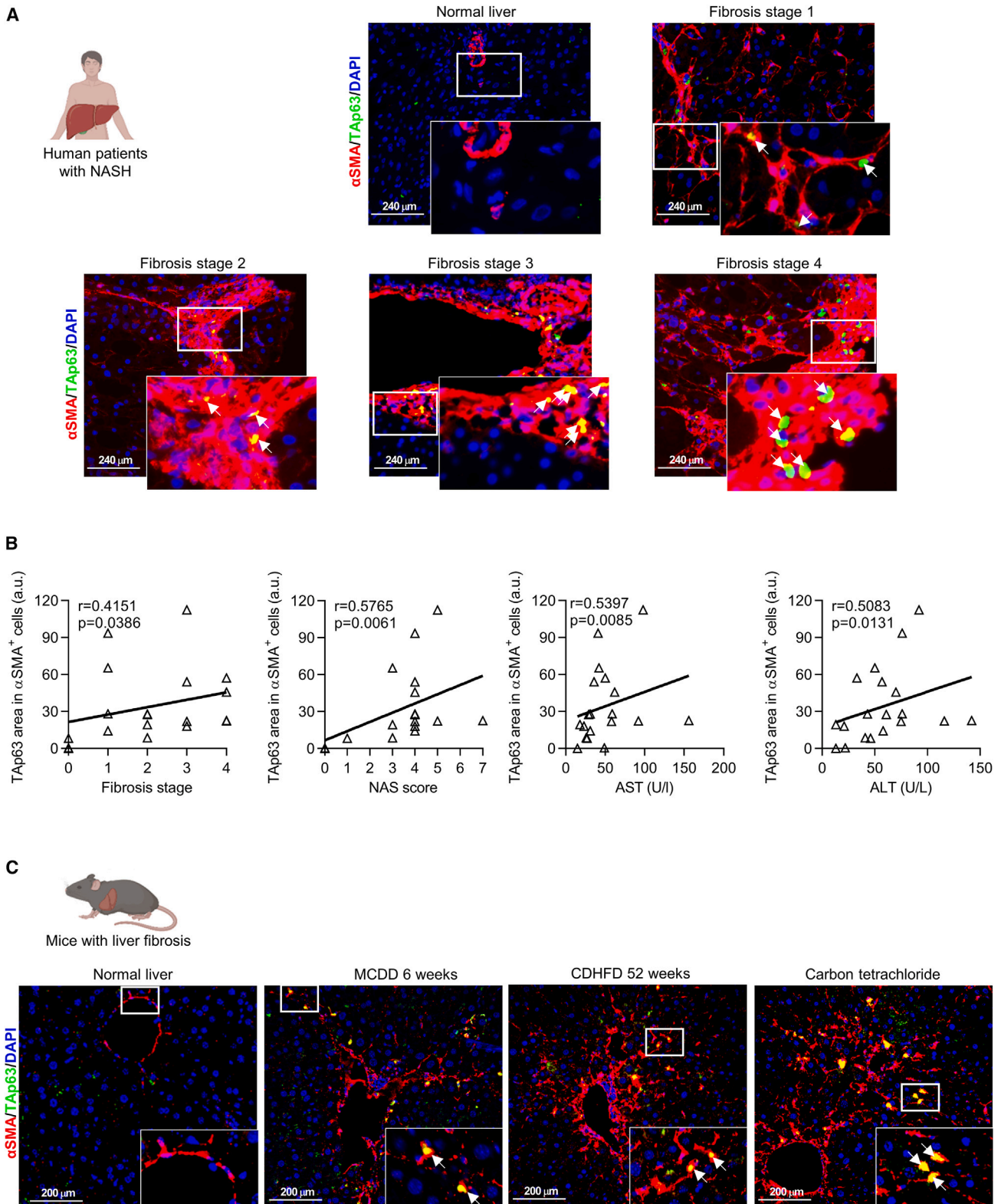
Figure 1. TAp63 protein is increased in activated hepatic stellate cells (HSCs) of livers with fibrosis

(A) Representative dual immunofluorescence for α-SMA (red) and TAp63 (green) in control subjects (n = 3) and NAFLD patients with different stages of fibrosis (n = 16). Nuclei were stained with DAPI (blue).

(legend continued on next page)

and prevention of senescence. In the dietary nonalcoholic steato-hepatitis (NASH) mouse model, TAp63 is induced in the liver, and its hepatic-specific knockdown ameliorates high-fat diet–induced steatosis by reducing endoplasmic reticulum stress and *de novo* lipogenesis.[9] In line with this, its overexpression accelerates the development of liver steatosis.[9] However, a potential direct role of TAp63 in liver fibrosis remains unstudied.

The key effectors in liver fibrosis are hepatic stellate cells (HSCs), which account for approximately 8%–14% of total cells in a healthy liver. In response to liver injury, HSCs move from a quiescent phenotype rich in vitamin A into activated myofibroblast-like cells with proliferative and migratory properties, a process defined as transdifferentiation.[10–12] Activation of HSCs is considered a crucial event that promotes increased extracellular matrix production and hepatic fibrosis, leading to the increased risk of hepatocarcinoma development.[13] It is reported that HSCs activation relies, at least partially, on a direct role of acetyl coenzyme A (CoA) carboxylase (ACC) by stimulating *de novo* synthesis of fatty acids.[14] Specifically, ACC1 catalyzes the rate-limiting step of *de novo* lipogenesis, conversion of acetyl CoA to malonyl-CoA, and an ACC inhibitor called GS-0976 is in clinical trials for the treatment of NASH.[15–18]

In the present study, we show that TAp63 levels were increased in HSCs from patients and animal models of NASH and liver fibrosis. The specific deletion of TAp63 in HSCs protected the mice against liver fibrosis. Overexpression of TAp63 in HSCs promotes their activation by inducing human epidermal growth factor receptor 2 (HER2) expression and thereby ACC1 and mitochondrial activity, whereas its silencing blunts transforming growth factor β1 (TGF-β1)-induced HSC activation. These findings indicate that TAp63 plays a critical role in the activation of HSCs, with implications in liver fibrosis development.

RESULTS

TAp63 is increased in activated HSCs from patients and mice with fibrosis

Immunofluorescence labeling in liver sections of control subjects and NAFLD patients (anthropometric characteristics in Table S1) showed that the TAp63, the most abundant isoform of p63, co-localized with α-smooth muscle actin (α-SMA) in the liver of NAFLD patients but not in the livers of control subjects (Figure 1A). Furthermore, the area of colocalization positively correlated with fibrosis stage, NAFLD activity score (NAS), and serum levels of AST and ALT (Figure 1B) (Spearman correlation test). Correlation of TAp63-αSMA area with other variables is available in Table S2. These results show that TAp63 is highly expressed in activated HSCs and in proportion to the fibrosis stage.

We next investigated the immunofluorescence of hepatic TAp63 in mice models of NASH and liver fibrosis. Specifically, we used mice fed a methionine- and choline-deficient diet (MCDD) for 6 weeks, mice fed a high-fat diet combined with choline deficiency (CDHFD) for 52 weeks, and mice treated with CCl₄. We found increased staining of TAp63 in α-SMA⁺ cells in these three mouse models, compared to normal livers (Figure 1C). Overall, these results indicate that TAp63 protein levels are consistently elevated in fibrosis in activated HSCs in both humans and mice.

p63 is upregulated in activated primary cultures of stellate cells from murine models and humans

We next examined p63 mRNA expression in primary mouse HSCs (PmHSCs) isolated from different mice models of fibrosis. p63 was consistently upregulated in activated PmHSCs from mice fed an MCDD for 6 weeks or fed a CDHFD for 52 weeks, or from mice treated with CCl₄, in comparison to the quiescent PmHSCs obtained from the control groups (Figures 2A–2C).

We then analyzed p63 expression in the process of tension-mediated activation of HSCs in culture. Quiescent HSCs were harvested from the livers of healthy rats, cultured on plates, and allowed to activate over the course of 7 days. Stellate cells cultured on uncoated rigid plastic plates become activated within days, expressing fibrogenic markers such as collagen I, proliferating and losing the retinoid-containing droplets as reported elsewhere,[19] and is widely used to study molecular mechanisms[20] and metabolic transformation[14] during the activation of primary stellate cells in culture. In parallel to the upregulation of fibrogenic markers, primary rat HSCs (PrHSCs) showed progressively increased levels of p63 expression (Figure 2D).

To assess whether p63 expression also changed during the activation of human HSCs, we treated primary human HSCs (PhHSCs) with TGF-β1, a potent fibrogenic inducer. Notably, TGF-β1 increased the expression of p63 as well as that of the profibrotic markers ACTA2, COL1α1, and COL1α2 (Figure 2E). We obtained similar results with the human LX-2 cells, a widely used HSC cell line for fibrosis[21]; in this case, the administration of TGF-β1 increased the mRNA expression of total p63, which reflects a specific increase in TAp63 but not ΔNp63, promoting consequently elevated proteins of TAp63 together with profibrotic markers (ACTA2, COL1α1, and COL1α2) in a time-dependent manner (Figure 2F). Overall, these results indicated that TAp63 is consistently elevated in activated HSCs in both humans and rodents.

HSC-specific depletion of TAp63 protects against liver fibrosis in mice

Given that specifically TAp63 protein levels are increased in human and murine HSCs, we next evaluated the potential effects of the depletion of TAp63 in HSCs in a mouse model of liver fibrosis. To this aim, we crossed TAp63-floxed mice with bacterial artificial chromosome transgenic mice, in which Cre expression is driven by lecithin-retinol acyltransferase,[22] to generate mice with a TAp63 knockout specifically in HSCs (HSC-TAp63-KO). To induce liver fibrotic NASH, mice were fed a CDHFD

(B) Correlations of TAp63-stained area in α-SMA⁺ cells with fibrosis stage, NAS score, and serum AST and ALT levels (Spearman correlation test).

(C) Representative dual immunofluorescence for α-SMA and TAp63 in liver sections from mice fed an MCDD for 6 weeks (n = 4), a CDHFD for 52 weeks (n = 4), or treated with carbon tetrachloride (0.6 mL/kg intraperitoneally [i.p.]) once per week for 6 weeks (n = 4). Untreated mice fed a standard chow diet were used as control group (n = 4).
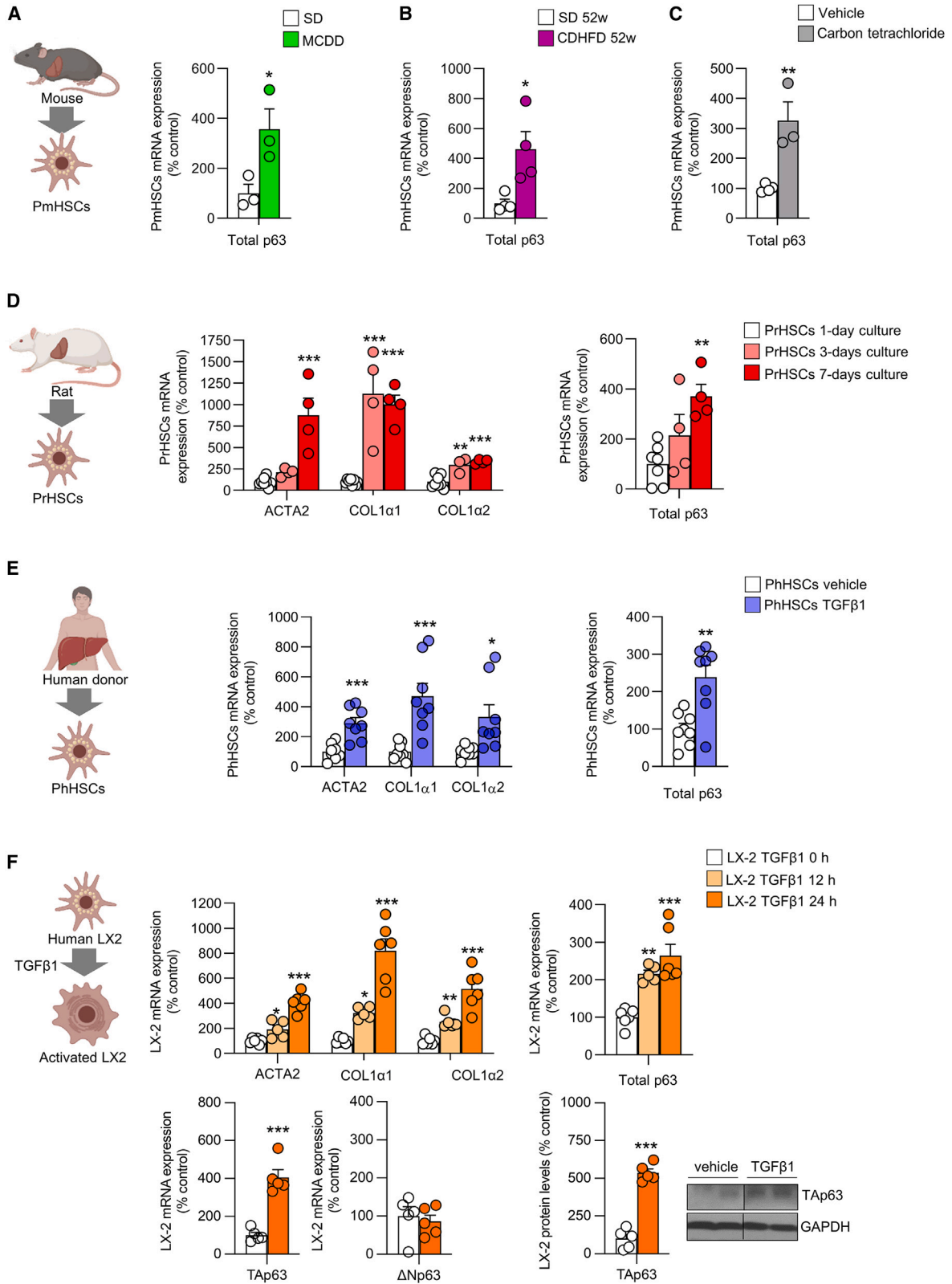
(legend on next page)

for 20 weeks. The depletion of TAp63 in HSCs significantly attenuated CDHFD-induced serum AST and hepatic collagen deposition, without affecting lipid accumulation (Figures 3A–3C). Likewise, HSC-TAp63-KO mice had reduced hepatic hydroxyproline levels and lower expression of fibrotic markers as compared to the control group (Figures 3B–3D). Similar results were obtained in mice fed an MCDD, with a reduction in AST, collagen deposition, hydroxyproline levels, and expression of fibrosis markers in HSC-TAp63-KO mice, compared to the wild-type (WT) group (Figures 3E–3H). More important, we did not detect changes in liver Ki67 and cleaved caspase-3 immunohistochemistry staining area (Figures S1A and S1B), or in serum levels of triglycerides, nonesterified fatty acids, and cholesterol (Table S3) between WT and HSC-TAp63-KO mice subjected to the two models of liver fibrosis. The efficiency of the stellate cell–specific deletion of TAp63 was corroborated by immunofluorescence, showing TAp63 staining colocalization with α-SMA in MCDD-fed WT mice but not in HSC-TAp63-KO mice, whereas TAp63 was found in albumin-positive cells in both genotypes (Figure S1C). This suggests that the observed fibrotic changes were independent of hepatic proliferation, liver apoptosis, and serum lipid alterations. Together, our results indicate that the absence of TAp63 in HSCs protects against fibrosis development.

Inhibition of p63 blocks *in vitro* HSC activation

Once we demonstrated that (1) TAp63 expression is induced in activated HSCs, (2) HSCs-specific depletion of TAp63 in mice can ameliorate liver fibrosis, and (3) that changes in total p63 specifically reflect variations in the predominant isoform TAp63, we next investigated whether p63 directly mediates the mechanisms governing HSCs activation. We silenced p63 expression with small interfering RNA (siRNA) against p63 (sip63) in TGF-β1-induced activated PhHSCs. TGF-β1 treatment in PhHSCs increased the mRNA expression of p63 (Figure S2A), the oxygen consumption rate (OCR), and the extracellular acidification rate (ECAR), indicative of mitochondrial and glycolytic functions, respectively (Figures 4A–4C, S2B, and S2C). p63 inhibition strongly reduced the TGF-β1-induced increases of OCR and ECAR (Figures 4A–4C, S2B, and S2C). Quantification of the different metabolic parameters of mitochondrial and glycolytic functions revealed that sip63 blunted TGF-β1-induced basal respiration, ATP-linked respiration, maximal respiration, and nonmitochondrial respiration, as well as basal and compensatory glycolysis (Figures S2B and S2C). Furthermore, cells with downregulated p63 showed suppressed levels of the TGF-β1-induced HSC activation markers (Figure 4D). Similar to the re-

sults obtained in PhHSCs, inhibition of p63 in LX-2 cells almost completely suppressed the increase in OCR and ECAR and the expression of activation markers following TGF-β1 administration (Figures 4E–4H, S3A, and S3C).

We next aimed to determine the underlying mechanism through which p63 exerts its effects on HSC activation. It is widely reported that p63 controls the expression and protein levels of different genes involved in *de novo* lipogenesis, mediating part of its metabolic and proliferative actions.[4,9,23–26] For this, we measured the mRNA expression of different markers of *de novo* lipogenesis in TGF-β1-activated LX-2 cells with or without silencing p63. We found that the silencing of p63 led to a significant decrease in ACC1 expression, without affecting the expression of other genes involved in *de novo* lipogenesis, such as fatty acid synthase (FAS), stearoyl-CoA desaturase-1 (SCD1) or sterol regulatory element binding protein 1c, or other proteins involved in lipolysis, particularly peroxisome proliferator activated receptor α, peroxisome proliferator-activated receptor gamma coactivator 1α, carnitine palmitoyltransferase 1A, carnitine palmitoyltransferase 2, long-chain acyl-CoA dehydrogenase, medium-chain acyl-CoA dehydrogenase, and short-chain acyl-CoA dehydrogenase (Figure 4I). Interestingly, ACC1 plays a key role orchestrating the energetic reprogramming of activated HSCs[14] and may constitute a target against fibrotic NASH.[14,18] In agreement with the reduced mRNA expression of ACC1 following the knockdown of p63, we found reduced enzymatic activity and protein levels of ACC1 (Figures 4J and 4K). We did not detect changes in the phosphorylated form of ACC (p-ACC) or in the protein levels of the phosphorylated (active) form of AMP-activated protein kinase α (AMPKα), suggesting that the reduced levels of ACC1 due to sip63 were independent of the AMPK pathway (Figures 4K and S3D). To note, no changes were found in levels of apoptotic, glycolytic, or proliferation markers (Figures S3E–S3G), indicating that the observed effects of sip63 on HSC activation occurred independently of apoptosis, regulation of expression of glycolytic enzymes, and cell proliferation. Altogether, these findings reveal that inhibition of p63 in HSCs diminished the metabolic and fibrogenic activation induced by TGF-β1.

Overexpression of TAp63 induces *in vitro* HSC activation

After demonstrating that TAp63 inhibition was sufficient to prevent HSC activation, we performed a gain-of-function experiment by overexpressing TAp63 in LX-2 cells to investigate whether this could activate HSCs. Our results showed that the ectopic expression of TAp63 (Figure 5A) stimulated the OCR and ECAR, indicative of an active and highly energetic phenotype (Figures 5B–5D). At the molecular level, TAp63

Figure 2. p63 is upregulated in activated primary cultures of stellate cells from murine models or human patients

(A) Levels of p63 mRNA in PmHSCs isolated from mice fed an MCDD for 6 weeks (n = 3) or (as a control) a standard diet (SD) for 6 weeks (n = 3).

(B and C) Mice fed a CDHFD (n = 4) or SD for 52 weeks (n = 4) (B), and (C) treated with carbon tetrachloride (0.6 mL/kg i.p.) (n = 3) or (as a control) with vehicle (n = 4) once per week for 6 weeks.

(D) mRNA expression of p63 and fibrogenesis markers in PrHSCs activated in culture (n = 4–8).

(E) Expression of fibrotic markers and p63 in PhHSCs from a donor following the administration of 8 ng/mL TGF-β1 for 24 h (n = 8).

(F) mRNA expression of fibrotic markers, total p63, TAp63, ΔNp63, and TAp63 protein levels in human LX-2 (n = 5–6) treated with TGF-β1 for 0, 12, or 24 h (n = 5–6). Hypoxanthine phosphoribosyltransferase (HPRT) and glyceraldehyde 3-phosphate dehydrogenase (GAPDH) were used to normalize mRNA and protein levels.

Data are mean ± SEM. *p < 0.05; **p < 0.01; ***p < 0.001.
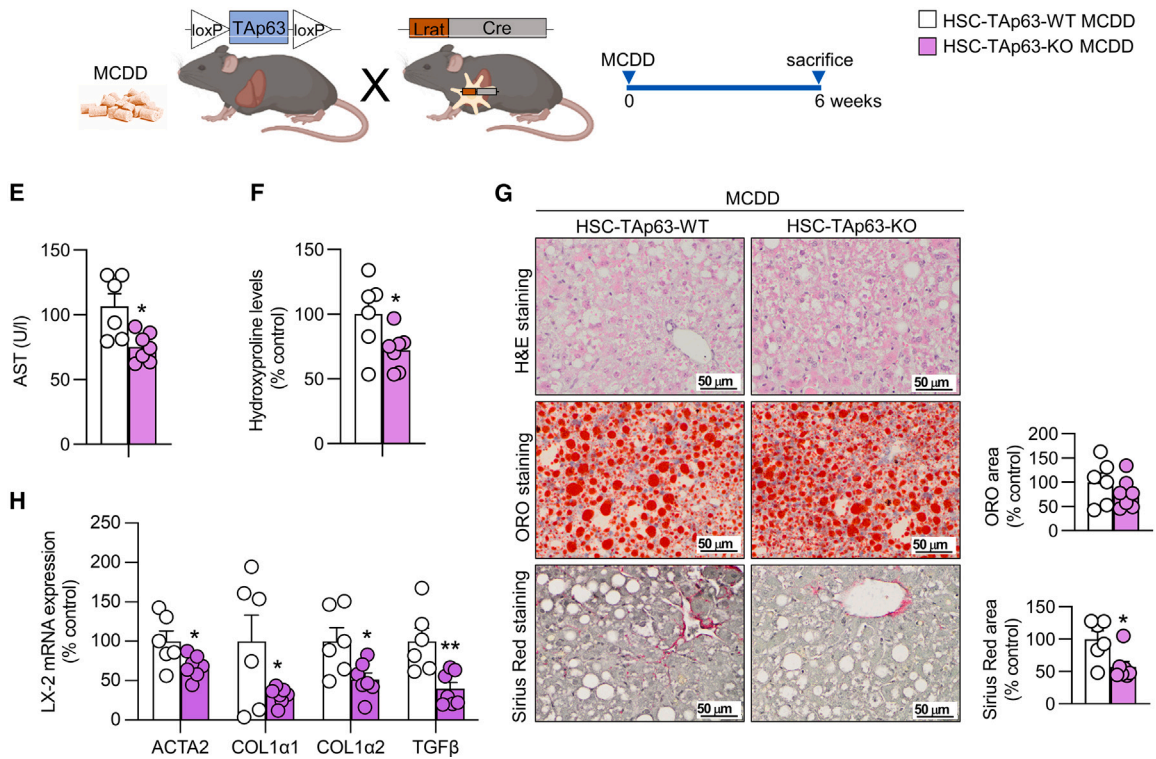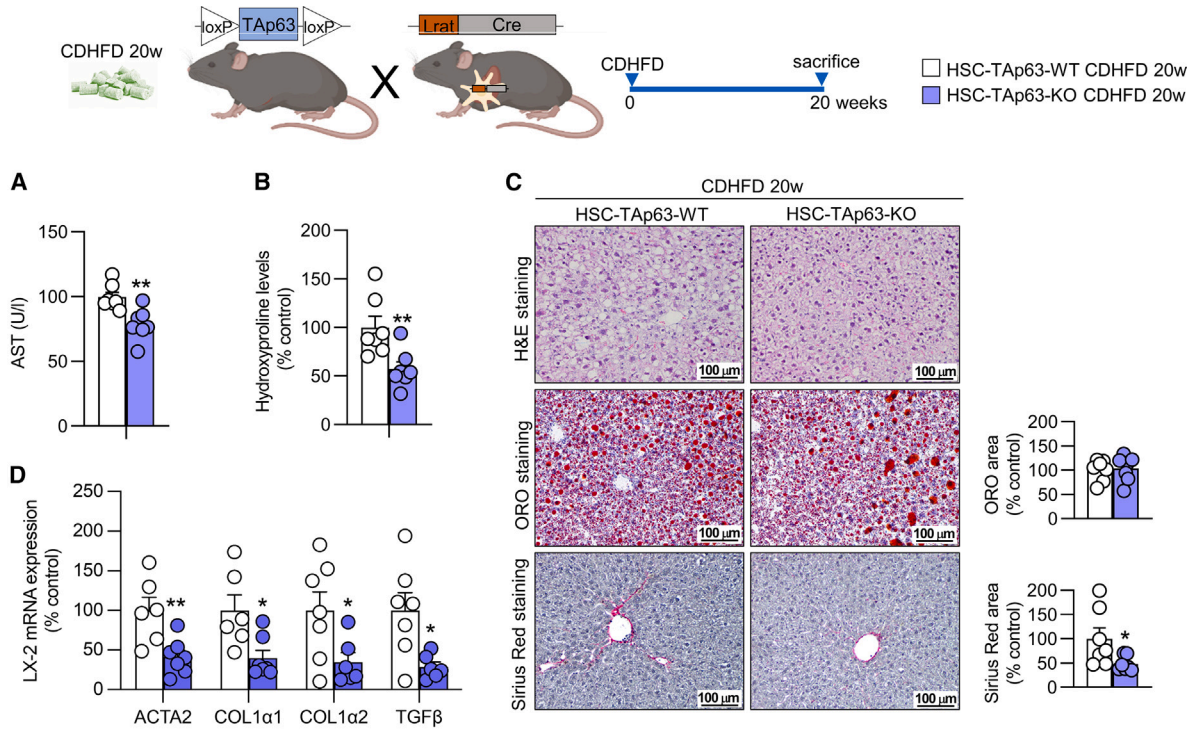
(legend on next page)

overexpression also increased mRNA and protein levels of ACC1 (Figures 5E and 5F) and the expression of fibrotic markers (Figure 5G). We did not detect changes in the expression of other markers of lipid metabolism or protein levels of p-ACC (Figures 5E and 5F). We also did not find changes in protein levels of apoptotic markers, expression of glycolytic markers, or proliferation, indicating that the observed effects of TAp63 on HSC activation occurred independently of apoptosis, transcriptional regulation of glycolysis, and cell proliferation (Figures S4A–S4C). Furthermore, to corroborate our previous results indicating that ΔNp63 is not involved in HSC activation and that only TAp63 reflects the effects of total p63 on HSC activity, we overexpressed the ΔNp63 isoform in HSCs, finding that this ΔN isoform did not affect the expression of ACC1 or HSC activation markers (Figure S4D). Our data indicated that ectopic expression of TAp63, but not ΔNp63, stimulated the metabolic and fibrogenic activation of HSCs.

Previous studies have implicated autophagy as a critical determinant of HSC activation by driving lipolysis.[27] Thus, we investigated whether the effects of p63 were dependent on autophagy. We initially measured the levels of well-established markers of autophagy in HSCs overexpressing TAp63 and failed to detect any significant change in the mRNA or protein levels of ATG5 and ATG7 (Figure S4E). Next, we monitored autophagic flux by analyzing light chain 3-II (LC3-II) turnover, in the presence or absence of the inhibitor of lysosome-mediated proteolysis, chloroquine (CQ), for 6 h. As expected, CQ administration induced LC3-II accumulation and the blockade of autophagy. Interestingly, LC3-II accumulation was induced to similar levels in both control plasmid- and TAp63 plasmid-treated cells, indicating that the LC3 flux was not altered by TAp63 (Figure S4F). Finally, we evaluated whether the inhibition of autophagy abrogates the impact of TAp63 on ACC1 and the induction of fibrosis. To this aim, LX-2 cells overexpressing TAp63 were treated with CQ. The overexpression of TAp63 led to the expected increased expression in ACC1, COL1α1, COl1α2, and ACTA2. These effects were not blocked by the administration of CQ (Figure S4G). Overall, all of these results indicate that the TAp63-induced ACC1 levels and fibrogenesis are not mediated via autophagy.

ACC1 mediates the *in vitro* HSC activation induced by TAp63

To evaluate the relevance of the ACC1-mediated actions of TAp63 in HSCs, we used the pharmacologic allosteric ACC1/ACC2 inhibitor GS-0976 (called firsocostat [FIR]), which is in clinical trials for the treatment of individuals with NASH and fibrosis.[18] LX-2 cells overexpressing TAp63 were incubated in medium supplemented with 0.5 μM FIR. After 24 h, TAp63 upregulation stimulated both ACC1 expression and ACC enzymatic activity; however, coadministration of FIR completely blocked these effects (Figure 6A). FIR also suppressed the increases of OCR and ECAR induced by TAp63, as shown in the mitochondrial and glycolytic flux assays (Figures 6B–6D and S5A). The subsequent quantification of metabolic parameters revealed a block in basal respiration, ATP-linked respiration, maximal respiration, and basal and compensatory glycolysis (Figure S5A). Moreover, the expression of fibrotic markers did not increase in LX-2 cells overexpressing TAp63 that were treated with FIR (Figure 6E). Similarly, genetic silencing of ACC1 by siRNA completely prevented TAp63 from stimulating ACC1 expression and enzymatic activity (Figure 6F), as well as mitochondrial and glycolytic functions (Figures 6G–6I and S5B), or from upregulating activation markers (Figure 6J). Along the same line, the quantification of metabolic parameters revealed that basal respiration, ATP-linked respiration, maximal respiration, and basal and compensatory glycolysis were blocked in LX-2 cells in which ACC1 had been downregulated (Figure S5B). Given the robust effect of TAp63 activity on ACC1 levels and the strong role of ACC1 in mediating the actions of TAp63 on HSC activation, we wanted to figure out whether TAp63 could directly regulate the transcriptional activity of ACC1. However, a luciferase reporter assay in the presence of TAp63 did not modify the activity of ACC1 promoter, suggesting that the TAp63-induced ACC1 levels could be indirect (Figure S5C). Overall, these data indicated that ACC1 mediates the effects of TAp63 in the metabolic and fibrogenic activation of HSCs, but TAp63 is not directly regulating ACC1 transcriptional expression.

HER2 regulates TAp63-induced ACC1 expression and HSC activation

To investigate in depth the mechanistic link between TAp63 and ACC1, we measured the expression of different known transcription factors controlling ACC1 expression, specifically ChREBP,[28] LXRa,[29] and HER2.[30] Since it was reported that ACC1 activity was induced in activated HSCs[14] and our results indicated that TAp63 also increased the expression and activity of ACC1, we measured the expression of ChREBP, LXRa, and HER2 in HSCs treated with TGF-β1. HER2 mRNA expression, but not ChREBP or LXRa, was upregulated by TGF-β1 and the genetic silencing of p63 blunted TGF-β1-induced HER2 expression (Figure 7A). In line with this, the overexpression of TAp63 in HSCs did not alter the levels of ChREBP and LXRa, but did

---

Figure 3. Deficiency of TAp63 in HSCs protects against liver fibrosis in mice fed a CDHFD

HSC-TAp63-KO or WT mice were fed a CDHFD for 20 weeks (n = 7).

(A) Serum levels of AST.

(B) Hepatic hydroxyproline levels.

(C) Liver sections stained with H&E (top), oil red O (center), and Sirius red (bottom). Staining areas were quantified.

(D) Expression of fibrosis markers in the liver. HSC-TAp63-KO or WT mice were fed an MCDD for 6 weeks (n = 6–7).
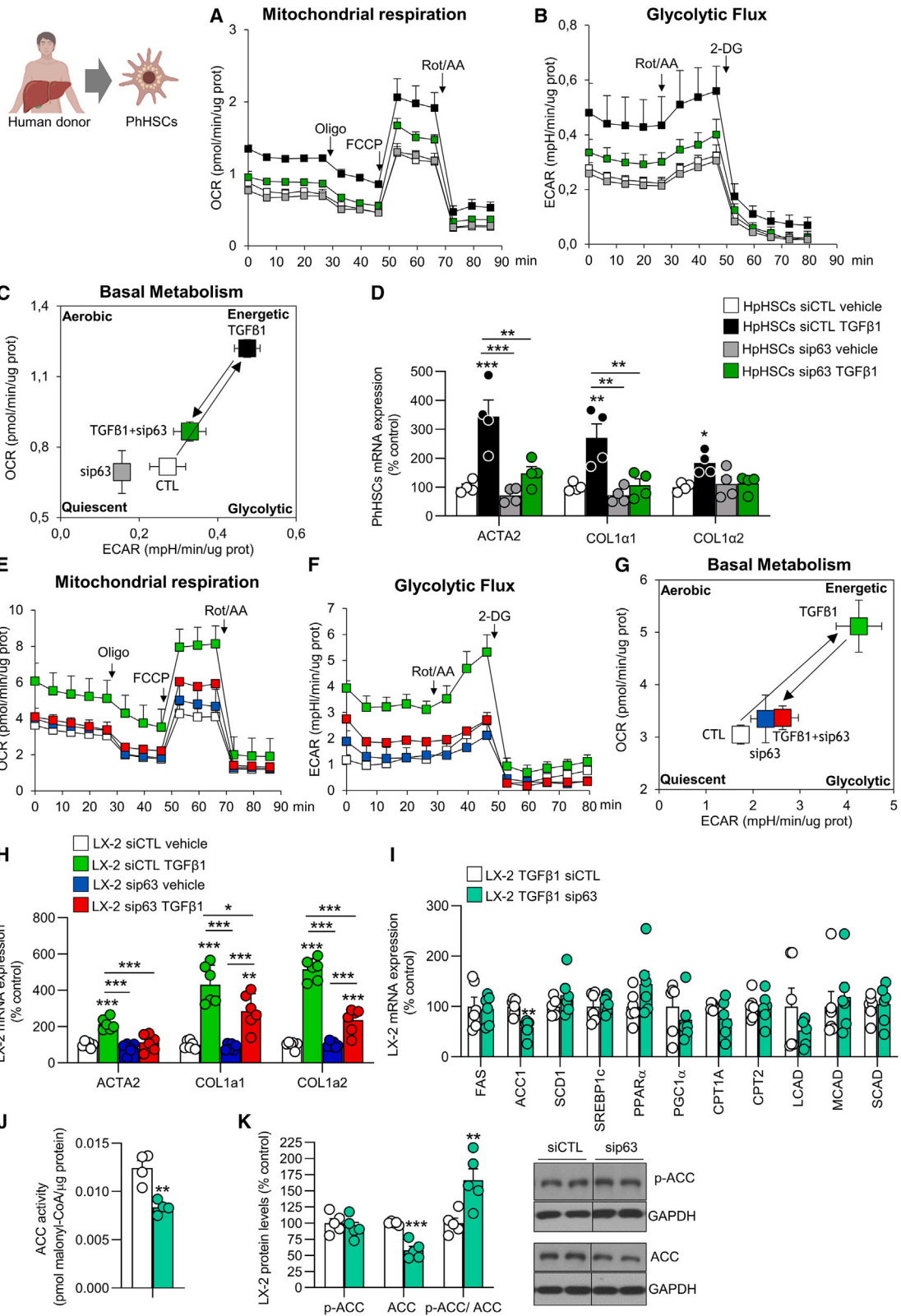
(E) Serum levels of AST.

(F) Hepatic hydroxyproline levels.

(G) Liver sections stained with H&E (top), oil red O (center), and Sirius red (bottom). Staining areas were quantified.

(H) Expression of fibrosis markers in the liver. HPRT was used to normalize mRNA levels.

Data are mean ± SEM. *p < 0.05; **p < 0.01.

See also Figure S1.

(legend on next page)

significantly increase HER2 mRNA (Figure 7B) and HER2 protein levels (Figure 7C). Finally, the genetic silencing of HER2 blunted the upregulation of ACC1 and fibrogenic markers in HSCs overexpressing TAp63 (Figures 7D–7F). Altogether, our results indicate that HER2 was positively regulated by TAp63 in HSCs and that HER2 mediates both TAp63-induced ACC1 expression and fibrogenic effect.

Three consensus elements for TAp63 are found in the first −1,600 bp upstream from the start transcription site in the Her2 promoter gene (http://alggen.lsi.upc.es/cgi-bin/promo_v3/promo/promoinit.cgi?dirDB=TF_8.3) (Figure 7G). To evaluate the possible transcriptional regulation of HER2 by TAp63, a luciferase reporter assay in the presence of TAp63 was carried out using plasmids containing the Her2 promoter region. LX-2 cells transfected with TAp63 significantly increased luciferase activity in the HER2 promoter fragment (Figure 7H).

We examined a public domain dataset containing single-cell RNA-sequencing (RNA-seq) data to find evidence of HER2 expression in human HSCs. To this end, we analyzed a recent single-cell RNA-seq dataset including people with normal liver and cirrhotic livers[31] and found that 191/2,094 cells (9.12%) were HER2$^+$ in the cirrhotic liver, in comparison with 122/892 cells (13.67%) HER2$^+$ in the normal liver. Despite the similar proportion of HSCs expressing HER2 in both cases, HER2 mRNA expression was very significantly increased in HSCs from the cirrhotic liver compared to HSCs from the normal liver (Figure 7I).

Next, we evaluated the expression of HER2 in primary human HSCs. We were able to detect baseline HER2 expression in HSCs, and its levels significantly increased after the treatment with TGF-β1 (Figure 7J). All of these data show that HSCs express HER2 and that their expression is induced upon activation.

Once the expression of HER2 in human HSCs was confirmed, we studied whether HER2 played a causal role in HSC activation and induction of fibrogenesis. For this, we performed experiments of gain- and loss-of-function of HER2 in vitro. We overexpressed HER2 by using a plasmid vector, as corroborated by qPCR and western blot (Figure S6A). In parallel to the upregulation of HER2, the mRNA expression of ACC1 and the fibrogenic markers ACTA2, COL1α1, and COL1α2 was also significantly induced (Figure S6B). Furthermore, the pharmacological inhibitor of HER2, namely CP724714, blocked the TAp63-induced activation of HSCs and ACC1 expression (Figure S6C).

TAp63 induced activation of HSCs is dependent on p53

The interaction between p53 and p63 is extremely complex and variable, as it is dependent on the cellular type and the status of the cells.[32] To address the relationship between p63 and p53 in HSCs, we measured the mRNA expression and protein level of p53 in LX-2 cells treated with TGF-β and found that p53 was significantly increased (Figure S7A). Moreover, p53 was significantly induced in LX-2 cells after the overexpression of TAp63 (Figure S7B). p53 protein levels were measured in LX-2 cells treated with TGF-β and silencing TAp63. The results indicated that TGF-β-induced p53 was blunted upon the inhibition of TAp63 (Figure S7C). Finally, to address the potential causal role of p53 in the profibrotic action of TAp63, we overexpressed TAp63 in LX-2 cells and silenced p53. The findings showed that the overexpression of TAp63 increased the mRNA expression of p53, ACC1, and fibrotic markers. However, in the group in which p53 was inhibited, the TAp63-induced expression of all of these genes was blunted (Figure S7D). All of these results demonstrate that p53 mediates the activation of HSCs induced by TAp63.

DISCUSSION

Mice with genetic deletion of p63 have profound developmental alterations that lead to early death.[33] In adult cells, the two classical functions of p63 are considered to be tumor suppression and cell maintenance and renewal[34]; however, it is now well established that p63 also regulates several metabolic pathways.[35] Our findings here expand our current knowledge about the metabolic actions of p63 and indicate that its expression is elevated in activated HSCs from rodent liver fibrosis models as well as in patients with liver fibrosis. Deletion of p63, and in particular, the TAp63 isoform, exclusively in HSCs has a protective fibrotic role. The importance of TAp63 in fibrosis development is in agreement with previous literature showing that hepatic TAp63 is highly expressed under the pathological conditions of fatty liver[9] and hepatocellular carcinoma.[36] Therefore, it seems that TAp63 could be involved in the progression of NAFLD until reaching tumorigenesis, a process that remains to be completely understood.[37] In this regard, it is also important to note that the involvement of p63 in the spectrum of NAFLD seems to be specifically linked to the TAp63 isoform because ΔNp63 lacks the TA domain and has the opposite effect as does TAp63.[38–40] Furthermore, ΔNp63 fails to change lipid content in hepatocytes[9] or to

---

Figure 4. Genetic inhibition of p63 attenuates the metabolic and fibrogenic activation induced by TGF-β1 in PhHSCs and human LX-2 cell line

(A and B) OCR (A) and (B) ECAR in PhHSCs silencing p63 and treated with TGF-β1 for 24 h. Arrows indicate the time point at which metabolic modulators (oligomycin [Oligo], phenylhydrazone [FCCP], rotenone/antimycin A [Rot/AA] and 2-deoxyglucose [2-DG]) were added to the assay. Parameters of mitochondrial and glycolytic function were calculated (n = 2–4).

(C) Graph depicting the effect of TGF-β1 or sip63 treatments on quiescent or energetic metabolic states, based on quantification of ECAR and OCR during basal metabolism.

(D) Expression of fibrotic markers (n = 4).

(E and F) OCR I and (F) ECAR in LX-2 cells silencing p63 and treated with TGF-β1 for 24 h.

(G) Basal energetic metabolic states, based on quantification of ECAR and OCR during basal metabolism (n = 4–6).
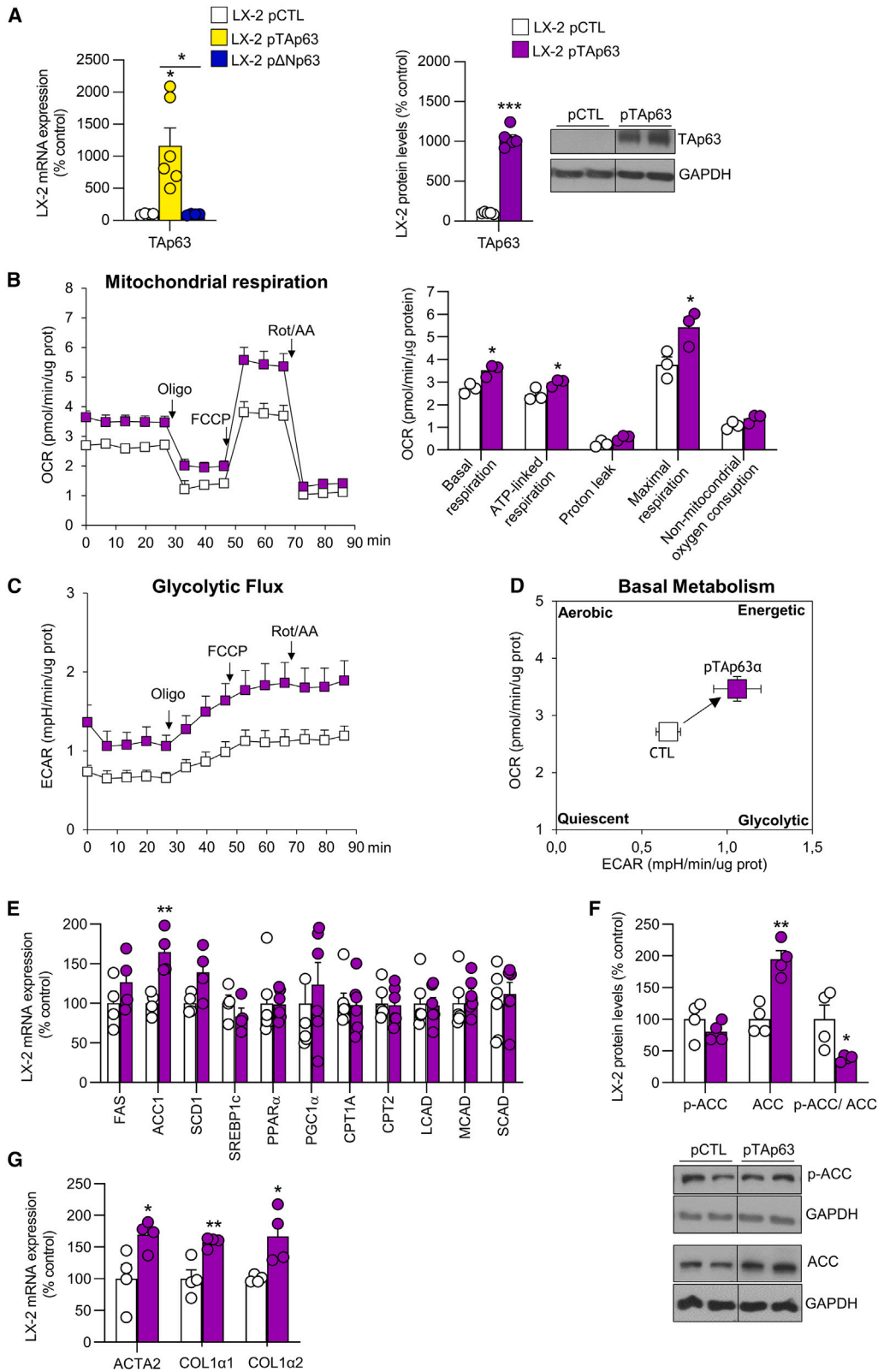
(H) Expression of fibrotic markers (n = 6).

(I) Expression of markers of lipid metabolism (n = 6).

(J and K) ACC activity (n = 4) (J), and (K) protein levels of ACC and p-ACC (n = 5) in LX-2 cells silencing p63 and treated with TGF-β1. HPRT and GAPDH were used to normalize mRNA and protein levels.

Data are mean ± SEM. *p < 0.05; **p < 0.01; ***p < 0.001.

See also Figures S2 and S3.

(legend on next page)

have any effects on fibrogenesis of stellate cells. This is likely consistent with the fact that the expression of TAp63 and ΔNp63 are regulated by different mechanisms in hepatocellular carcinoma cell lines.[41]

Our results indicated that the effects of TAp63 in liver fibrosis are mediated via rewiring energy metabolism in HSCs, as demonstrated by strong changes in mitochondrial respiration, glycolytic flux, and fatty acid metabolism following the manipulation of TAp63. Indeed, activated HSCs require energy obtained from oxidative phosphorylation, and this is correlated with a higher number of mitochondria[42] as well as with increased mitochondrial activity.[43] HSC activation has also been shown to require glycolysis.[42] In addition, fatty acid metabolism, and in particular, *de novo* lipogenesis, is a critical feature in the activation of HSCs. For instance, the *in vitro* or *in vivo* inhibition of ACC1 directly blocks HSC activation, displaying antifibrotic activity.[14] In agreement with this, l-α-lysophosphatidylinositol (LPI), which also favors the progression of fibrosis, induces the increase of ACC in HSCs, and the inhibition of this enzyme blocks LPI-induced HSC activation and liver damage.[44] In line with the relevant role of *de novo* lipogenesis in HSC activation, aramchol, which is in Phase IIb clinical trials to treat NASH,[45] downregulates SCD1 in HSCs and attenuates cellular fibrogenesis.[46] Our findings in HSCs showed that silencing TAp63 decreased mitochondrial function, glycolytic activity, and ACC1 activity, whereas TAp63 overexpression induced mitochondrial respiration, glycolytic flux, and ACC1 activity. The blockade of ACC1 by genetic or pharmacological tools completely blunted the ability of HSCs to activate oxidative phosphorylation and glycolysis in response to TAp63 overexpression and also normalized the expression of fibrotic markers. This agrees with different reports describing a role for ACC and *de novo* lipogenesis as modulators of glycolysis, mitochondrial function, and cell activation. In particular, ACC inhibition in HSCs suppressed the activation of glycolysis and oxidative phosphorylation induced by TGF-β1.[14] Similarly, lung fibroblasts required FAS to become activated *in vitro*, and FAS inhibition blocked pulmonary fibrosis *in vivo*.[47] In the present study we showed that the modulation of glycolytic rate induced by TAp63 via ACC1 is independent of a direct transcriptional regulation of glycolytic makers. The mechanism by which the inhibition of *de novo* lipogenesis blocks glycolysis in HSCs remains unknown. Of note, although TAp63 regulates the rewiring of lipid metabolism in activated stellate cells, the depletion of p63 in HSCs *in vivo* did not alter the metabolic flux of serum lipids. This apparent discrepancy of our results compared to other publications reporting that the ACC inhibition may increase serum triglycerides levels could be explained by the target specificity;

whereas our approach targeted TAp63 specifically in HSCs, the other studies targeted ACC in the whole liver, with an obvious dominant action of hepatocytes,[18] or directly targeted ACC in the hepatocytes.[48] Together, these findings suggest that *de novo* lipogenesis may be used generally during the metabolic reprogramming underlying stellate cell activation.

Our data indicating that ACC1 mediates the fibrogenic actions of TAp63 support the pivotal role for TAp63 on fatty acid metabolism in a variety of contexts. Previous reports described that this transcription factor stimulates the expression of lipogenic enzymes that favor liver steatosis[9] and also promotes cell survival through FAS.[25] Besides the direct transcriptional actions, TAp63 is also able to modulate the activity of enzymes involved in fatty acid metabolism via AMPK. In particular, TAp63 regulates the expression of AMPK, which controls the activity of ACC through inhibitory phosphorylation.[24] In the present study, we found that TAp63 overexpression induced increases in the enzymatic activity and protein and mRNA levels of ACC1, whereas its knockdown reduced the activity, protein levels, and expression of ACC1. However, TAp63 did not induce the transcriptional activity of ACC1 in LX-2 cells, and the factor linking TAp63 to ACC1 seems to be HER2. For instance, TAp63 triggered the transcriptional activity of HER2 and its downregulation or pharmacological inhibition, avoiding TAp63-induced ACC1 expression and fibrogenic activity. Interestingly, HER2 has been demonstrated to induce the expression of lipogenic enzymes in breast cancer cells, thereby favoring their survival and proliferation.[30] Indeed, in the present study, we found that HER2 was consistently overexpressed in HSCs from people with cirrhosis and HSCs from murine models of fibrosis, and the ectopic expression of HER2 in HSCs was sufficient to activate the cells. HER2 gains are potentially associated with NASH-induced hepatocellular carcinoma as assessed using a single-cell microfluorescence *in situ* hybridization approach.[49] The existence of a functional HER2-ACC1 axis also in HSCs supports the idea that this mechanism also plays a relevant role in the activation of HSCs. However, we did not detect changes in protein levels of phosphorylated ACC nor in the phosphorylated (active) form of AMPKα following the manipulation of TAp63. Together, our findings suggest that TAp63 controls ACC1 via HER2 rather than via AMPK.

Our results also highlight the cell-type-specific metabolic roles of p63; in the liver, the TAp63 expressed in hepatocytes promotes fatty acid storage, whereas TAp63 expressed in HSCs stimulates fibrosis. The cell-type-specific actions of p63 have also been observed in cancer.[50] Since liver tumor initiation is often linked to fibrosis caused by HSCs, our results may indicate that the increased levels of TAp63 in fibrosis could participate in

---

Figure 5. Overexpression of TAp63 activates human LX-2 cells

(A) mRNA expression of TAp63 and ΔNp63 (n = 4–6), and protein levels of TAp63 (n = 5–6) in LX-2 cell after overexpressing TAp63.

(B) OCR.

(C and D) ECAR (C) and (D) basal metabolism in LX-2 cells overexpressing TAp63 (n = 3). Arrows indicate the time point at which metabolic modulators (Oligo, FCCP, Rot/AA, and 2-DG) were added to the assay.

(E) Expression of markers of lipid metabolism (n = 4–6).

(F and G) Protein levels of ACC and p-ACC (n = 4) (F), and (G) mRNA levels of fibrogenic markers (n = 4). HPRT and GAPDH were used to normalize mRNA and protein levels.

Data are mean ± SEM. *p < 0.05; **p < 0.01; ***p < 0.001.

See also Figure S4.
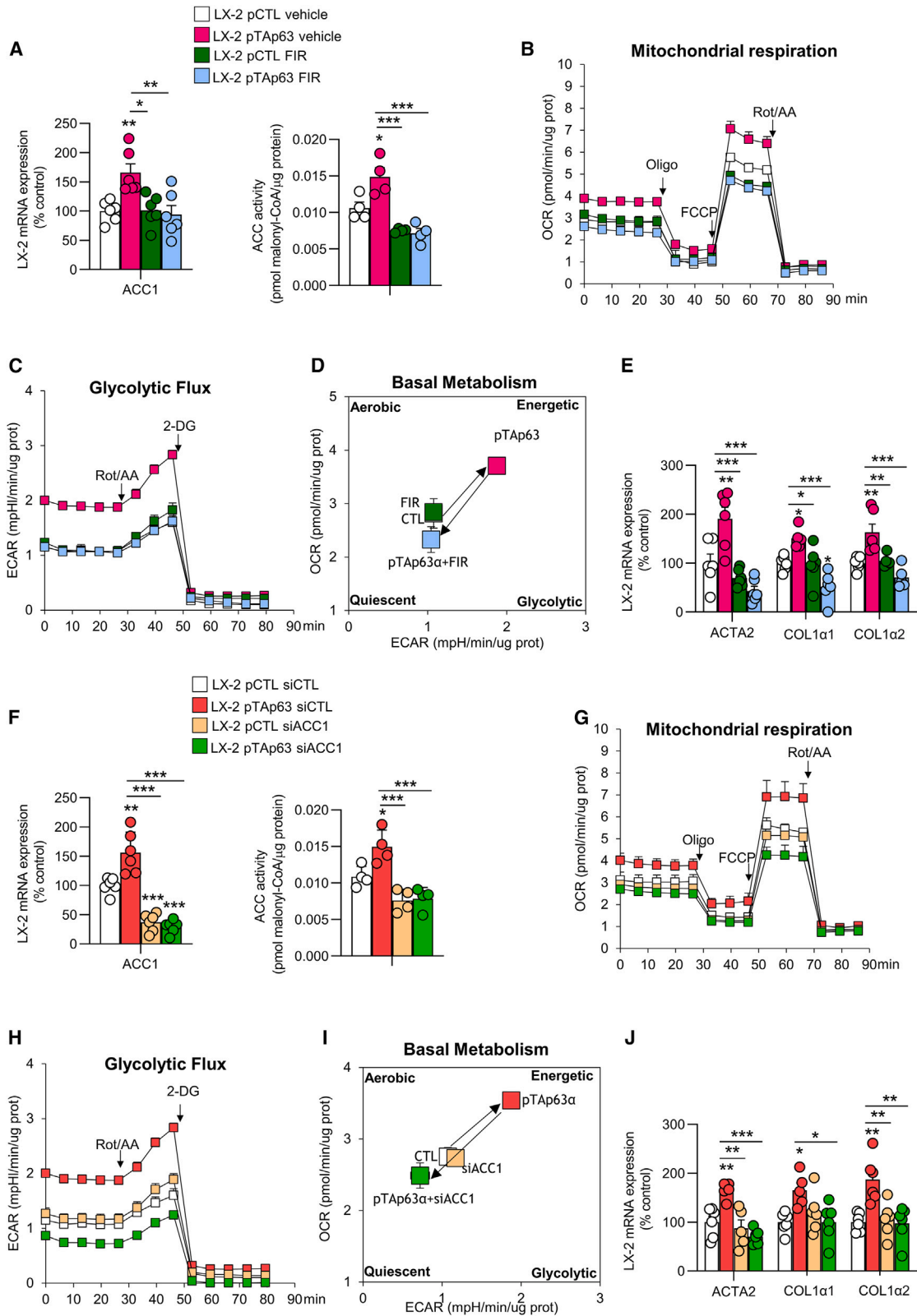
(legend on next page)

cancer progression, a process during which p63 is known to be highly expressed.[51] Of note, p63+ cells have also been identified in human cholangiocarcinoma and hepatocellular carcinoma.[52] An interesting point is that TAp63 seems to require p53 to activate HSCs. We found that both TAp63 and TGF-β induced protein levels of p53 and the silencing of p53 blunts TAp63-induced HSC activation. This is in line with previous research suggesting that p53 is overexpressed in 35% of samples in liver biopsies in patients with non-neoplastic liver disease, steatohepatitis, and chronic hepatitis.[53] Further in-depth studies will be necessary to decipher the mechanisms of this interaction because despite being part of the same family and showing structural similarities, the roles of these two proteins are not always redundant and can be different.[54,55] The most representative example is probably that, whereas p53-null mice develop normally and are viable, p63-null mice have severely affected development.[56,57] Therefore, the complex interactions between p53 family members are reflected by different functional implications.

Finally, our preclinical data are of potential clinical value because we found a significant positive correlation between TAp63 in activated HSCs and fibrosis stage in a well-characterized cohort of patients with NAFLD. Furthermore, TAp63 positively correlated with other parameters of liver injury, specifically NAS score and serum AST and ALT. In addition, when using primary human HSCs and the human LX-2 cell line, the results were very similar to those we observed in primary HSCs from mice and rats, with increased p63 expression in situations of fibrosis.

In summary, the results presented here implicate TAp63 in the progression of liver fibrosis in both humans and animal models and suggest that it induced a metabolic rewiring in HSCs, which involved triggering ACC1-HER2, mitochondrial function, and glycolysis. In addition, the inhibition of p63 in HSCs mitigated liver fibrosis *in vivo* and *in vitro*. Considering that fibrosis often precedes liver tumor development, this study offers new insight into TAp63-induced changes in the microenvironment of HSC activation and to how this could have potential consequences for tumor initiation.

Limitations of the study

Despite our *in vitro* findings pointing to a key role of HER2 in the regulation of fatty acid metabolism in HSCs, we have not tested whether the *in vivo* specific genetic manipulation of HER2 in HSCs is equally efficient. Further studies are needed to investigate whether HER2 maintains its capacity to modulate the transcriptional activity of ACC1 and affect liver fibrosis in animal

models. In line with this, additional studies are necessary to clearly elucidate the function of p53 as a regulator of the HER2/ACC1 signaling pathway in HSCs as discussed above.

STAR★METHODS

Detailed methods are provided in the online version of this paper and include the following:

- KEY RESOURCES TABLE
- RESOURCE AVAILABILITY
  - Lead contact
  - Materials availability
  - Data and code availability
- EXPERIMENTAL MODEL AND STUDY PARTICIPANT DETAILS
  - Human samples
  - Animals and diets
  - HSCs conditional knockout mice for TAp63
- METHOD DETAILS
  - Histological procedures
  - Hydroxyproline assay
  - Serum levels of metabolites
  - Isolation and culture of murine HSCs
  - Culture of primary human HSCs (PhHSCs)
  - Human LX-2 culture
  - *Gene silencing in primary human HSCs (PhHSCs)*
  - Gene silencing in LX-2 cells
  - Gene overexpression *in vitro*
  - Metabolic flux assays
  - TGFβ1 treatment
  - Firsocostat administration
  - CP724714 administration
  - Autophagic flux
  - ACC activity assay
  - Cell proliferation
  - *In vitro* luciferase assay in cells
  - Real-time PCR
  - Western blot
- QUANTIFICATION AND STATISTICAL ANALYSIS

SUPPLEMENTAL INFORMATION

Supplemental information can be found online at https://doi.org/10.1016/j.xcrm.2024.101401.

Figure 6. Pharmacological or genetic inhibition of ACC1 blunts the metabolic and fibrogenic activation induced by TAp63 in human HSCs

(A) ACC1 mRNA levels (n = 6) and ACC activity (n = 4) in LX-2 cells overexpressing TAp63 and treated with 0.5 μM FIR.

(B) OCR (n = 3).

(C) ECAR (n = 4). Arrows indicate the time point at which metabolic modulators (Oligo, FCCP, Rot/AA, and 2-DG) were added to the assay.

(D) Graph depicting the effect of overexpression of TAp63 and administration of FIR on quiescent or energetic metabolic states, based on quantification of ECAR and OCR during basal metabolism.

(E) Expression of fibrogenic markers (n = 6).

(F) ACC1 mRNA levels (n = 6) and ACC activity (n = 4) in LX-2 cells overexpressing TAp63 and silencing ACC1.
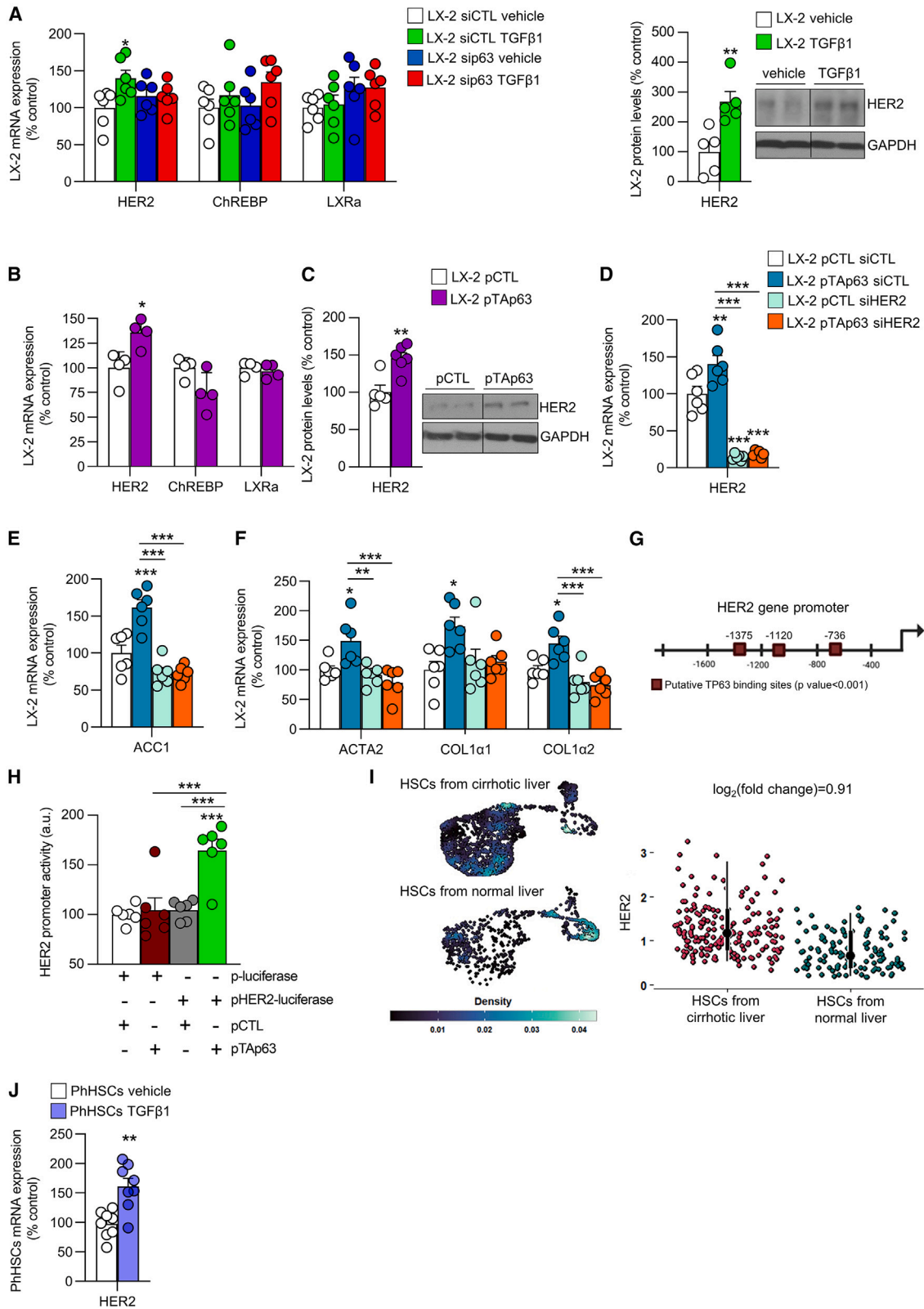
(G) OCR (n = 2–3).

(H) ECAR (n = 4).

(I) Basal metabolism.

(J) Expression of fibrogenic markers (n = 6). HPRT was used to normalize mRNA levels.

Data are mean ± SEM. *p < 0.05; **p < 0.01; ***p < 0.001.

See also Figure S5.

(legend on next page)

Cell Reports Medicine
Article

AUTHOR CONTRIBUTIONS

M.F.F., E.N., M.J.G.-R., U.F., B.P., T.P., C.R., A.W., M.V.-R., M.G.-V., M.P.C.-V., S.B.B., V.D., M.F.F., A.S., N.d.S.L., M.L., and V.H.: study conception and design, data acquisition, and data analysis and interpretation: M.F.F., C.D., V.P., M.S., P.I., J.C., M.L.M.-C., R.S., M.M., F.J.C., G.S., and R.N.: manuscript writing and final review.

DECLARATION OF INTERESTS

The authors declare no competing interests.

REFERENCES

1. Yang, A., Kaghad, M., Wang, Y., Gillett, E., Fleming, M.D., Dötsch, V., Andrews, N.C., Caput, D., and McKeon, F. (1998). p63, a p53 homolog at 3q27-29, encodes multiple products with transactivating, death-inducing, and dominant-negative activities. Mol. Cell *2*, 305–316.

2. Schmale, H., and Bamberger, C. (1997). A novel protein with strong homology to the tumor suppressor p53. Oncogene *15*, 1363–1367.

3. Levrero, M., De Laurenzi, V., Costanzo, A., Gong, J., Wang, J.Y., and Melino, G. (2000). The p53/p63/p73 family of transcription factors: overlapping and distinct functions. J. Cell Sci. *113 (Pt 10)*, 1661–1670.

4. Berkers, C.R., Maddocks, O.D.K., Cheung, E.C., Mor, I., and Vousden, K.H. (2013). Metabolic regulation by p53 family members. Cell Metabol. *18*, 617–633.

5. Mehta, S., Campbell, H., Drummond, C.J., Li, K., Murray, K., Slatter, T., Bourdon, J.C., and Braithwaite, A.W. (2021). Adaptive homeostasis and the p53 isoform network. EMBO Rep. *22*, e53085.

6. Krstic, J., Reinisch, I., Schupp, M., Schulz, T.J., and Prokesch, A. (2018). p53 Functions in Adipose Tissue Metabolism and Homeostasis. Int. J. Mol. Sci. *19*, 2622.

7. Khoury, M.P., and Bourdon, J.C. (2010). The isoforms of the p53 protein. Cold Spring Harbor Perspect. Biol. *2*, a000927.

8. Candi, E., Dinsdale, D., Rufini, A., Salomoni, P., Knight, R.A., Mueller, M., Krammer, P.H., and Melino, G. (2007). TAp63 and DeltaNp63 in cancer and epidermal development. Cell Cycle *6*, 274–285.

9. Porteiro, B., Fondevila, M.F., Delgado, T.C., Iglesias, C., Imbernon, M., Iruzubieta, P., Crespo, J., Zabala-Letona, A., Fernø, J., González-Terán, B., et al. (2017). Hepatic p63 regulates steatosis via IKKbeta/ER stress. Nat. Commun. *8*, 15111.

10. Loomba, R., Friedman, S.L., and Shulman, G.I. (2021). Mechanisms and disease consequences of nonalcoholic fatty liver disease. Cell *184*, 2537–2564.

11. Trivedi, P., Wang, S., and Friedman, S.L. (2021). The Power of Plasticity-Metabolic Regulation of Hepatic Stellate Cells. Cell Metabol. *33*, 242–257.

12. Kisseleva, T., and Brenner, D. (2021). Molecular and cellular mechanisms of liver fibrosis and its regression. Nat. Rev. Gastroenterol. Hepatol. *18*, 151–166.

13. Guarino, M., Bovet, C., and Dufour, J.F. (2019). When lifestyles sign. Hepatobiliary Surg. Nutr. *8*, 69–71.

14. Bates, J., Vijayakumar, A., Ghoshal, S., Marchand, B., Yi, S., Kornyeyev, D., Zagorska, A., Hollenback, D., Walker, K., Liu, K., et al. (2020). Acetyl-CoA carboxylase inhibition disrupts metabolic reprogramming during hepatic stellate cell activation. J. Hepatol. *73*, 896–905.

15. Loomba, R., Kayali, Z., Noureddin, M., Ruane, P., Lawitz, E.J., Bennett, M., Wang, L., Harting, E., Tarrant, J.M., McColgan, B.J., et al. (2018). GS-0976 Reduces Hepatic Steatosis and Fibrosis Markers in Patients With Nonalcoholic Fatty Liver Disease. Gastroenterology *155*, 1463–1473.e6.

16. Lawitz, E.J., Coste, A., Poordad, F., Alkhouri, N., Loo, N., McColgan, B.J., Tarrant, J.M., Nguyen, T., Han, L., Chung, C., et al. (2018). Acetyl-CoA Carboxylase Inhibitor GS-0976 for 12 Weeks Reduces Hepatic De Novo Lipogenesis and Steatosis in Patients With Nonalcoholic Steatohepatitis. Clin. Gastroenterol. Hepatol. *16*, 1983–1991.e3.

17. Parlati, L., Régnier, M., Guillou, H., and Postic, C. (2021). New targets for NAFLD. JHEP Rep. *3*, 100346.

18. Loomba, R., Noureddin, M., Kowdley, K.V., Kohli, A., Sheikh, A., Neff, G., Bhandari, B.R., Gunn, N., Caldwell, S.H., Goodman, Z., et al. (2021). Combination Therapies Including Cilofexor and Firsocostat for Bridging Fibrosis and Cirrhosis Attributable to NASH. Hepatology *73*, 625–643.

Figure 7. Genetic inhibition of HER2 blocks the fibrogenic activation induced by TAp63 in human HSCs

(A and B) mRNA levels of different transcription factors known to regulate ACC1 expression in LX-2 cells (A) treated with TGF-β1 and silencing p63 (n = 6) and (B) overexpressing TAp63 (n = 4).

(C) Protein levels of HER2 in LX-2 cells treated with TGF-β1 for 24 h and overexpressing TAp63 are also shown (n = 5–6) (see also A).

(D) mRNA expression of HER2.

(E and F) ACC1 (E) and (F) fibrogenic markers in LX-2 cells overexpressing TAp63 following the silencing of HER2 (n = 6).

(G) Diagram depicting putative binding sites for TAp63 in the HER2 gene promoter.

(H) Levels of HER2 promoter activity in LX-2 cells transfected with TAp63 (n = 6).

(I) Nebulosa plots of the HER2 density in the uniform manifold approximation and projection visualization of cirrhotic HSCs (n = 4) and normal HSCs (n = 4). HER2 expressions in both conditions are also shown.

(J) Expression of HER2 in primary human HSCs treated with TGF-β1 (n = 8). HPRT and GAPDH were used to normalize mRNA and protein levels.

Data are mean ± SEM. *p < 0.05; **p < 0.01; ***p < 0.001.

See also Figures S6 and S7.

19. Friedman, S.L., Roll, F.J., Boyles, J., Arenson, D.M., and Bissell, D.M. (1989). Maintenance of differentiated phenotype of cultured rat hepatic lipocytes by basement membrane matrix. J. Biol. Chem. *264*, 10756–10762.

20. De Minicis, S., Seki, E., Uchinami, H., Kluwe, J., Zhang, Y., Brenner, D.A., and Schwabe, R.F. (2007). Gene expression profiles during hepatic stellate cell activation in culture and in vivo. Gastroenterology *132*, 1937–1946.

21. Xu, L., Hui, A.Y., Albanis, E., Arthur, M.J., O'Byrne, S.M., Blaner, W.S., Mukherjee, P., Friedman, S.L., and Eng, F.J. (2005). Human hepatic stellate cell lines, LX-1 and LX-2: new tools for analysis of hepatic fibrosis. Gut *54*, 142–151.

22. Mederacke, I., Hsu, C.C., Troeger, J.S., Huebener, P., Mu, X., Dapito, D.H., Pradere, J.P., and Schwabe, R.F. (2013). Fate tracing reveals hepatic stellate cells as dominant contributors to liver fibrosis independent of its aetiology. Nat. Commun. *4*, 2823.

23. Liao, W., Liu, H., Zhang, Y., Jung, J.H., Chen, J., Su, X., Kim, Y.C., Flores, E.R., Wang, S.M., Czarny-Ratajczak, M., et al. (2017). Ccdc3: A New P63 Target Involved in Regulation Of Liver Lipid Metabolism. Sci. Rep. *7*, 9020.

24. Su, X., Gi, Y.J., Chakravarti, D., Chan, I.L., Zhang, A., Xia, X., Tsai, K.Y., and Flores, E.R. (2012). TAp63 is a master transcriptional regulator of lipid and glucose metabolism. Cell Metabol. *16*, 511–525.

25. Sabbisetti, V., Di Napoli, A., Seeley, A., Amato, A.M., O'Regan, E., Ghebremichael, M., Loda, M., and Signoretti, S. (2009). p63 promotes cell survival through fatty acid synthase. PLoS One *4*, e5877.

26. Huang, Y., Bell, L.N., Okamura, J., Kim, M.S., Mohney, R.P., Guerrero-Preston, R., and Ratovitski, E.A. (2012). Phospho-ΔNp63α/SREBF1 protein interactions: bridging cell metabolism and cisplatin chemoresistance. Cell Cycle *11*, 3810–3827.

27. Tsuchida, T., and Friedman, S.L. (2017). Mechanisms of hepatic stellate cell activation. Nat. Rev. Gastroenterol. Hepatol. *14*, 397–411.

28. Dentin, R., Benhamed, F., Hainault, I., Fauveau, V., Foufelle, F., Dyck, J.R.B., Girard, J., and Postic, C. (2006). Liver-specific inhibition of ChREBP improves hepatic steatosis and insulin resistance in ob/ob mice. Diabetes *55*, 2159–2170.

29. Talukdar, S., and Hillgartner, F.B. (2006). The mechanism mediating the activation of acetyl-coenzyme A carboxylase-alpha gene transcription by the liver X receptor agonist T0-901317. J. Lipid Res. *47*, 2451–2461.

30. Yoon, S., Lee, M.Y., Park, S.W., Moon, J.S., Koh, Y.K., Ahn, Y.H., Park, B.W., and Kim, K.S. (2007). Up-regulation of acetyl-CoA carboxylase alpha and fatty acid synthase by human epidermal growth factor receptor 2 at the translational level in breast cancer cells. J. Biol. Chem. *282*, 26122–26131.

31. Filliol, A., Saito, Y., Nair, A., Dapito, D.H., Yu, L.X., Ravichandra, A., Bhattacharjee, S., Affo, S., Fujiwara, N., Su, H., et al. (2022). Opposing roles of hepatic stellate cell subpopulations in hepatocarcinogenesis. Nature *610*, 356–365.

32. Melino, G. (2011). p63 is a suppressor of tumorigenesis and metastasis interacting with mutant p53. Cell Death Differ. *18*, 1487–1499.

33. Keyes, W.M., Wu, Y., Vogel, H., Guo, X., Lowe, S.W., and Mills, A.A. (2005). p63 deficiency activates a program of cellular senescence and leads to accelerated aging. Genes Dev. *19*, 1986–1999.

34. Costanzo, A., Pediconi, N., Narcisi, A., Guerrieri, F., Belloni, L., Fausti, F., Botti, E., and Levrero, M. (2014). TP63 and TP73 in cancer, an unresolved "family" puzzle of complexity, redundancy and hierarchy. FEBS Lett. *588*, 2590–2599.

35. Candi, E., Smirnov, A., Panatta, E., Lena, A.M., Novelli, F., Mancini, M., Viticchiè, G., Piro, M.C., Di Daniele, N., Annicchiarico-Petruzzelli, M., and Melino, G. (2017). Metabolic pathways regulated by p63. Biochem. Biophys. Res. Commun. *482*, 440–444.

36. Glickman, J.N., Yang, A., Shahsafaei, A., McKeon, F., and Odze, R.D. (2001). Expression of p53-related protein p63 in the gastrointestinal tract and in esophageal metaplastic and neoplastic disorders. Hum. Pathol. *32*, 1157–1165.

37. Klein, S., and Dufour, J.F. (2017). Nonalcoholic fatty liver disease and hepatocellular carcinoma. Hepat. Oncol. *4*, 83–98.

38. Westfall, M.D., Mays, D.J., Sniezek, J.C., and Pietenpol, J.A. (2003). The Delta Np63 alpha phosphoprotein binds the p21 and 14-3-3 sigma promoters in vivo and has transcriptional repressor activity that is reduced by Hay-Wells syndrome-derived mutations. Mol. Cell Biol. *23*, 2264–2276.

39. Senoo, M., Matsumura, Y., and Habu, S. (2002). TAp63gamma (p51A) and dNp63alpha (p73L), two major isoforms of the p63 gene, exert opposite effects on the vascular endothelial growth factor (VEGF) gene expression. Oncogene *21*, 2455–2465.

40. Candi, E., Rufini, A., Terrinoni, A., Dinsdale, D., Ranalli, M., Paradisi, A., De Laurenzi, V., Spagnoli, L.G., Catani, M.V., Ramadan, S., et al. (2006). Differential roles of p63 isoforms in epidermal development: selective genetic complementation in p63 null mice. Cell Death Differ. *13*, 1037–1047.

41. Petitjean, A., Cavard, C., Shi, H., Tribollet, V., Hainaut, P., and Caron de Fromentel, C. (2005). The expression of TA and DeltaNp63 are regulated by different mechanisms in liver cells. Oncogene *24*, 512–519.

42. Chen, Y., Choi, S.S., Michelotti, G.A., Chan, I.S., Swiderska-Syn, M., Karaca, G.F., Xie, G., Moylan, C.A., Garibaldi, F., Premont, R., et al. (2012). Hedgehog controls hepatic stellate cell fate by regulating metabolism. Gastroenterology *143*, 1319–1329.e11.

43. Gajendiran, P., Vega, L.I., Itoh, K., Sesaki, H., Vakili, M.R., Lavasanifar, A., Hong, K., Mezey, E., and Ganapathy-Kanniappan, S. (2018). Elevated mitochondrial activity distinguishes fibrogenic hepatic stellate cells and sensitizes for selective inhibition by mitotropic doxorubicin. J. Cell Mol. Med. *22*, 2210–2219.

44. Fondevila, M.F., Fernandez, U., Gonzalez-Rellan, M.J., Da Silva Lima, N., Buque, X., Gonzalez-Rodriguez, A., Alonso, C., Iruarrizaga-Lejarreta, M., Delgado, T.C., Varela-Rey, M., et al. (2021). The L-alpha-Lysophosphatidylinositol/G Protein-Coupled Receptor 55 System Induces the Development of Nonalcoholic Steatosis and Steatohepatitis. Hepatology *73*, 606–624.

45. Ratziu, V., de Guevara, L., Safadi, R., Poordad, F., Fuster, F., Flores-Figueroa, J., Arrese, M., Fracanzani, A.L., Ben Bashat, D., Lackner, K., et al. (2021). Aramchol in patients with nonalcoholic steatohepatitis: a randomized, double-blind, placebo-controlled phase 2b trial. Nat. Med. *27*, 1825–1835.

46. Bhattacharya, D., Basta, B., Mato, J.M., Craig, A., Fernández-Ramos, D., Lopitz-Otsoa, F., Tsvirkun, D., Hayardeny, L., Chandar, V., Schwartz, R.E., et al. (2021). Aramchol downregulates stearoyl CoA-desaturase 1 in hepatic stellate cells to attenuate cellular fibrogenesis. JHEP Rep. *3*, 100237.

47. Jung, M.Y., Kang, J.H., Hernandez, D.M., Yin, X., Andrianifahanana, M., Wang, Y., Gonzalez-Guerrico, A., Limper, A.H., Lupu, R., and Leof, E.B. (2018). Fatty acid synthase is required for profibrotic TGF-β signaling. Faseb. J. *32*, 3803–3815.

48. Kim, C.W., Addy, C., Kusunoki, J., Anderson, N.N., Deja, S., Fu, X., Burgess, S.C., Li, C., Ruddy, M., Chakravarthy, M., et al. (2017). Acetyl CoA Carboxylase Inhibition Reduces Hepatic Steatosis but Elevates Plasma Triglycerides in Mice and Humans: A Bedside to Bench Investigation. Cell Metabol. *26*, 394–406.e6.

49. Döring, P., Calvisi, D.F., and Dombrowski, F. (2021). Nuclear ErbB2 expression in hepatocytes in liver disease. Virchows Arch. *478*, 309–318.

50. Moses, M.A., George, A.L., Sakakibara, N., Mahmood, K., Ponnamperuma, R.M., King, K.E., and Weinberg, W.C. (2019). Molecular Mechanisms of p63-Mediated Squamous Cancer Pathogenesis. Int. J. Mol. Sci. *20*, 3590.

51. Steurer, S., Riemann, C., Büscheck, F., Luebke, A.M., Kluth, M., Hube-Magg, C., Hinsch, A., Höflmayer, D., Weidemann, S., Fraune, C., et al. (2021). p63 expression in human tumors and normal tissues: a tissue microarray study on 10,200 tumors. Biomark. Res. *9*, 7.

52. Ramalho, F.S., Ramalho, L.N.Z., Della Porta, L., and Zucoloto, S. (2006). Comparative immunohistochemical expression of p63 in human

cholangiocarcinoma and hepatocellular carcinoma. J. Gastroenterol. Hepatol. *21*, 1276–1280.

53. Akyol, G., Dursun, A., Poyraz, A., Uluoglu, O., Ataoglu, O., Edalý, N., and Memis, L. (1999). P53 and proliferating cell nuclear antigen (PCNA) expression in non-tumoral liver diseases. Pathol. Int. *49*, 214–221.

54. Woodstock, D.L., Sammons, M.A., and Fischer, M. (2021). p63 and p53: Collaborative Partners or Dueling Rivals? Front. Cell Dev. Biol. *9*, 701986.

55. Dötsch, V., Bernassola, F., Coutandin, D., Candi, E., and Melino, G. (2010). p63 and p73, the ancestors of p53. Cold Spring Harbor Perspect. Biol. *2*, a004887.

56. Mills, A.A., Zheng, B., Wang, X.J., Vogel, H., Roop, D.R., and Bradley, A. (1999). p63 is a p53 homologue required for limb and epidermal morphogenesis. Nature *398*, 708–713.

57. Yang, A., Schweitzer, R., Sun, D., Kaghad, M., Walker, N., Bronson, R.T., Tabin, C., Sharpe, A., Caput, D., Crum, C., and McKeon, F. (1999). p63 is essential for regenerative proliferation in limb, craniofacial and epithelial development. Nature *398*, 714–718.

58. Zubiete-Franco, I., Fernández-Tussy, P., Barbier-Torres, L., Simon, J., Fernández-Ramos, D., Lopitz-Otsoa, F., Gutiérrez-de Juan, V., de Dava-

lillo, S.L., Duce, A.M., Iruzubieta, P., et al. (2017). Deregulated neddylation in liver fibrosis. Hepatology *65*, 694–709.

59. Chatterjee, A., Upadhyay, S., Chang, X., Nagpal, J.K., Trink, B., and Sidransky, D. (2008). U-box-type ubiquitin E4 ligase, UFD2a attenuates cisplatin mediated degradation of DeltaNp63alpha. Cell Cycle *7*, 1231–1237.

60. Li, Y.M., Pan, Y., Wei, Y., Cheng, X., Zhou, B.P., Tan, M., Zhou, X., Xia, W., Hortobagyi, G.N., Yu, D., and Hung, M.C. (2004). Upregulation of CXCR4 is essential for HER2-mediated tumor metastasis. Cancer Cell *6*, 459–469.

61. Kleiner, D.E., Brunt, E.M., Van Natta, M., Behling, C., Contos, M.J., Cummings, O.W., Ferrell, L.D., Liu, Y.C., Torbenson, M.S., Unalp-Arida, A., et al. (2005). Design and validation of a histological scoring system for nonalcoholic fatty liver disease. Hepatology *41*, 1313–1321.

62. Leffert, H.L., Koch, K.S., Moran, T., and Williams, M. (1979). Liver cells. Methods Enzymol. *58*, 536–544.

63. Zubiete-Franco, I., García-Rodríguez, J.L., Martínez-Uña, M., Martínez-Lopez, N., Woodhoo, A., Juan, V.G.D., Beraza, N., Lage-Medina, S., Andrade, F., Fernandez, M.L., et al. (2016). Methionine and S-adenosylmethionine levels are critical regulators of PP2A activity modulating lipophagy during steatosis. J. Hepatol. *64*, 409–418.

STAR★METHODS

KEY RESOURCES TABLE

REAGENT or RESOURCE	SOURCE	IDENTIFIER
Antibodies		
Acetyl-CoA carboxylase, ACC	Abcam	Cat# ab45174; RRID:AB_867475
Phospho- acetyl-Coa Carboxylase (Ser 79), pACC	Cell Signaling	Cat# 3661; RRID:AB_330337
Phospho-AMPKα (Thr172)	Cell Signaling	Cat# 2535; RRID:AB_331250
Cleaved caspase 3	Cell Signaling	Cat# 9664; RRID:AB_2070042
Cleaved caspase 7	Cell Signaling	Cat# 9491; RRID:AB_2068144
Glyceraldehyde 3- phosphate dehydrogenase, GAPDH	Merck	Cat# CB1001
HER2/ErbB2 (29D8)	Cell Signaling	Cat# 2165; RRID:AB_10692490
TAp63	Biolegend	Cat# 938102
p53	Cell Signaling	Cat# 2527; RRID:AB_10695803
APG5/ATG5	Santa Cruz	Cat# sc-133158; RRID:AB_2243288
ATG7 (EPR6251)	Abcam	Cat# ab133528; RRID:AB_2532126
LC3A/B	Cell Signaling	Cat# 4108; RRID:AB_2137703
HSP90 (AC-16)	Santa Cruz	Cat# sc-101494; RRID:AB_1124018
Chemicals, peptides, and recombinant proteins		
Carbon tetrachloride	Strem Chemicals	Cat# 06-3545
TGFβ1	PreproTech	Cat# 100-21
Firsocostat	MedChemExpress	Cat# HY-16901
CP724714	Sigma-Aldrich	Cat# PZ-0335
Chloroquine	Sigma-Aldrich	Cat# H0915
Critical commercial assays		
Hydroxyproline Assay Kit	Merck	Cat# MAK008
AST activity Kit	Spinreact	Cat# 41273
Mouse Malonyl coenzyme A ELISA Kit	MyBioSource	Cat#MBS705127
MTT Test	Merck	Cat# M2003
Deposited data		
Raw and analyzed data	This paper	N/A
Experimental models: Cell lines		
Human: LX-2 HSC	Merck	Cat# SCC064; RRID:CVCL_5792
Human: Primary Stellate Cells (PhHSCs)	Lonza	Cat# HUCLS-1M
Experimental models: Organisms/strains		
Mouse: B6.Cg-Tg(Lrat-cre)1Rshw/Mmjax	Schwabe, R.F.[58]	Cat# 069595-JAX; RRID:MMRRC_069595-JAX
Oligonucleotides		
siGENOME SMARTPool p63	Dharmacon	Cat# L-003330-00-0005
siGENOME SMARTPool ACC1	Dharmacon	Cat# L-004551-00-0005
siGENOME SMARTPool HER2	Dharmacon	Cat# L-003126-00-0005
siGENOME SMARTPool Non -Targeting	Dharmacon	Cat# D-001206-13-05
Primers for XX, see Table S4	This paper	N/A
Recombinant DNA		
Plasmid: Tap63alpha-FLAG	David Sidransky[59]	RRID:Addgene_27008
Plasmid: deltaNp63alpha-FLAG	David Sidransky[59]	RRID:Addgene_26979
Plasmid: HER2 wt	Mien-Chie Hung[60]	RRID:Addgene_16257
Plasmid: p-luciferase/HER2/ACC1	Vector builder	N/A

(Continued on next page)

Continued

REAGENT or RESOURCE	SOURCE	IDENTIFIER
Software and algorithms		
ImageJ 1.52p software	Schneider et al.	https://imagej.nih.gov/ij/
Prism Software Version 8.0.2 (GraphPad)	Dotmatics	https://www.graphpad.com/features
Agilent Seahorse Analytics 1.0.0–520	Agilent	https://www.agilent.com/en/product/cell-analysis/real-time-cell-metabolic-analysis/xf-software/agilent-seahorse-analytics-787485#technology

RESOURCE AVAILABILITY

Lead contact
Further information and requests for resources should be directed to and will be fulfilled by the lead contact, Ruben Nogueiras (ruben.nogueiras@usc.es).

Materials availability
This study did not generate new unique reagents.

Data and code availability
- All data reported in this paper will be shared by the lead contact upon request.
- This paper does not report original code.
- Any additional information required to reanalyze the data reported in this paper is available from the lead contact upon request.

EXPERIMENTAL MODEL AND STUDY PARTICIPANT DETAILS

Human samples
The study population included 16 NAFLD patients who underwent a liver biopsy according to the routine decisions in the clinical practice or at the time of bariatric surgery in Marqués de Valdecilla University Hospital (Santander, Spain). Inclusion criteria for NAFLD patients were based on an alcohol intake lesser than 30 g/day for men and lesser than 20 g/day for women, the presence of biopsy-proven steatosis with/without necroinflammation and/or fibrosis, and no evidence of hepatitis B and/or C virus infection as well as human immunodeficiency virus (HIV) infection. Hepatic histopathological analysis was performed according to the scoring system of Kleiner et al.[61] Four histopathological features will be semi-quantitatively evaluated: grade of steatosis (0, <5%; 1, 5%–30%; 2, >30%–60%; 3, >60%), lobular inflammation (0, no inflammatory foci; 1, <2 inflammatory foci per 200x field; 2, 2–4 inflammatory foci per 200x field; 3, >4 inflammatory foci per 200x field), hepatocellular ballooning (0, none; 1, few balloon cells; 2, many cells/prominent ballooning), and stage of fibrosis (from 0, none to 4, cirrhosis). The characteristics of NAFLD patients are described in Table S1. Liver samples with histologically normal liver (NL) obtained from 3 subjects during bariatric surgery were used as subject controls (mean age 38.3 ± 5.2 and BMI 46.9 ± 4.4).

The study was performed in agreement with the Declaration of Helsinki, and with local and national laws. The Cantabria's Research Ethics Committee approved the study procedures (internal code: 2018.139 and 2019.087). All the study subjects signed the corresponding written informed consent.

Animals and diets
8 weeks old male C57BL/6J mice were housed in air-conditioned rooms (22°C–24°C) under a 12:12 h light/dark cycle and had *ad libitum* access to standard diet (SD), methionine-and choline-deficient diet (MCDD) (A02082002BR, Research Diets), choline-deficient and high fat diet (CDHFD) (D05010402; 45% fat, Research Diets) for the specified times. Carbon tetrachloride (06–3545, Strem Chemicals) was administered by i.p. injection at a dose of 0.6 mL/kg once a week for 6 weeks to induce liver fibrosis in mice, using corn oil as vehicle.[58] Animal experiments were conducted in accordance with the standards approved by the Faculty Animal Committee at the University of Santiago de Compostela, and the experiments were performed in agreement with the Rules of Laboratory Animal Care and International Law on Animal Experimentation.

HSCs conditional knockout mice for TAp63
The ablation of TAp63 in the HSCs was obtained in our lab by crossing TAp63-floxed mice with Lecithin retinol acyltransferase (Lrat)-Cre mice,[22] resulting in mice with Cre recombinase expression under the control of Lrat (HSCs specific) promotor.

METHOD DETAILS

Histological procedures
Oil Red O staining
Frozen liver samples were cut in 8μm sections with a cryostat and stained in filtered Oil Red O for 10 min. After being washed in distilled water, sections were counterstained with Mayer's hematoxylin for 3 min and mounted in aqueous mounting (glycerin jelly).

Hematoxylin and Eosin and staining
Liver samples were fixed in 4% formaldehyde for 24 h and then dehydrated and embedded in paraffin. Sections of 4μm were cut with a microtome and stained using a standard Hematoxylin and Eosin alcoholic procedure according to the manufacturer's instructions (BioOptica). Then, sections were rinsed with distilled water, dried at 37°C for 30 min and mounted with permanent (non-alcohol, non-xylene based) mounting media.

Sirius Red staining
Samples fixated in paraffin were dewaxed, hydrated and stained in PicroSirius staining red for 1 h. Then, samples were washed with distilled water, dehydrated in three changes of 100% ethanol and cleared in xylene and mounted in a resinous medium. In these three histological staining techniques, up to 4 representative microphotographs of each animal were taken with a BX51 microscope equipped with a DP70 digital camera (Olympus). Lipids in Oil Red O- stained sections, collagen depositions in Sirius Red-stained sections and positive area in immunohistochemistry were quantified using ImageJ 1.52p software.

Immunohistochemistry
For ki67 and cleaved caspase 3 inmunohistochemistry staining, samples fixated in paraffin were dewaxed, hydrated, pre-treated in PTLink TE buffer pH 9 and blocked with 3% peroxidase for 10 min. Sections were then incubated with the primary antibody (dakoM7248, DAKO, 1:500) (9664, Cell Signaling, 1:100) overnight and at room temperature, followed by an incubation with the secondary antibody (EnVision, DAKO) for 30 min at room temperature. After that, DAB developer was used for 1 min and sections were counterstained with Mayer's hematoxylin for 10 min, dehydrated and mounted.

Immunofluorescence
For TAp63-αSMA and TAp63-Albumin immunofluorescence staining, samples dewax were pre-treated in PTLink Citrate Buffer pH 6. Next, sections were washed three times in TBS 0.1M for 5 min and incubated in blocking solution (2% donkey serum +0.3% Triton X-100 + 0.25% BSA) in TBS 0.1M for 60 min. Then, sections were incubated with the primary antibodies TAp63 (938102, Biolegend) (1:500) and αSMA (ab124964, Abcam) (1:200) and Albumin (ab7940, Abcam) (1:200) in blocking solution for 24 h at 4°C. After incubation with the primary antibody, sections were rinsed with TBS 0.1M three times for 5 min each and then incubated in the solution (0.3% Triton X-100 + 0.25% BSA in TBS 0.1M) with the secondary antibodies: Cy3 donkey anti-rabbit (711-165-152, Jackson ImmunoResearch Labs) and Cy5 donkey anti-mouse (715-175-151, Jackson ImmunoResearch Labs) (1:1000) or Alexa 555 anti-Sheep (A21436, Thermo) (1:1000) for 60 min at room temperature. Sections were then washed and coverslipped with Fluorogel coverslip mounting solution.

In these three immunostaining techniques, up to 7 representative microphotographs of each human sample (up to 4, in the case of animal samples) was taken with a Thunder Imager tissue microscope (Leica Microsystems). Leica Las X 3.7.4 software was used for acquisition and analysis of immunohistochemistry/immunofluorescence staining. ImageJ 1.52p software was used for the quantification of the staining area.

Hydroxyproline assay
Hepatic collagen content was evaluated by measuring the levels of hepatic hydroxyproline with the Hydroxyproline Assay Kit (MAK008, MERCK) following the manufacturer's instructions. Briefly, liver samples were hydrolyzed in concentrated hydrochloric acid at 120°C for 3 h, and evaporated to dryness under vacuum. We added chloramine T/oxidation buffer mixture and incubated it for 5 min at room temperature, then DMAB reagent for 90 min at 60°C. Absorbance was read at 560 nm and the amount of hydroxyproline was calculated against the standard curve concentration.

Serum levels of metabolites
During the sacrifice of mice, whole trunk blood was collected and then spun for 15 min at 6000xg and 4°C. The supernatant was transferred to a new tube to obtain the serum. AST activity (41273, Spinreact) was measured by spectrophotometry in a ThermoScientific Multiskan GO spectrophotometer.

Isolation and culture of murine HSCs
Both primary mouse HSCs (PmHSCs) and primary rat HSCs (PrHSCs) were obtained by *in situ* perfusion of the liver with collagenase digestion following the Lefferts method.[62] To isolate PpmHSCs, male BALB/cByJ mice were anesthetized with isoflurane (in O₂), the abdomen was opened, and a catheter was inserted into the cava vein. Liver was perfused with buffer 1 [Leffert buffer, 1 mM EGTA] (37°C, oxygenated) and portal vein was cut. Subsequently, liver was perfused with buffer 2 [Leffert buffer] and buffer 3 [Leffert buffer, 2 mM CaCl₂, 1 g/L collagenase type I (Worthington)] (37°C, oxygenated). After the perfusion, liver was placed in a Petri dish containing buffer 2 supplemented with 1% BSA and disaggregated with forceps. Digested liver was filtered through sterile gauze. Then, HSCs were isolated either from healthy control, mice treated with carbon

tetrachloride, mice fed an MCDD or mice fed a CDHFD as previously described.[58] Briefly, after hepatic disaggregation, cell suspension was differentially-centrifuged at 400 rpm for 2 min. Hepatocytes-enriched pellet was removed and parenchymal cell-enriched supernatant was subjected to a density Percoll gradient (24% on top of 32%) (Percoll Plus, GE Healthcare) and selective adherence. The fraction enriched in HSCs was cultured in RPMI 1640 medium without serum and supplemented with 1% Antibiotic-Antimycotic (15240062, Gibco) overnight. Finally, the medium was replaced with fresh medium supplemented with 20% FBS for 24 h, and PmHSCs were collected for mRNA extraction. To obtain PrHSCs, a Sprague-Dawley rat was used. After the isolation of PrHSCs by density gradient followed by selective adherence, cells were kept in RPMI 1640 medium without serum overnight. Then, the medium was replaced with fresh medium supplemented with 20% FBS. Activation of PrHSCs was induced by the maintenance in culture for 1, 3 or 7 days. At these time points, PrHSCs were collected for mRNA extraction.

Culture of primary human HSCs (PhHSCs)
PhHSCs (HUCLS1, Lonza) were cultured in collagen I-coated plates and maintained in Human Stellate Growth Medium (MCST250, Lonza), at 37°C in a humidified atmosphere containing 5% CO_2, following the manufacturer's instructions.

Human LX-2 culture
The human LX-2 HSC line (SCC064, MERCK) was grown in Dulbecco's Modified Eagle's Medium (DMEM) high glucose (D5796, MERCK) supplemented with 2% (v/v) FBS and 1% (v/v) Glutamine-Penicillin-Streptomycin solution.[21]

Gene silencing in primary human HSCs (PhHSCs)
Primary human HSCs (PhHSCs) were transfected with specific small-interference RNA (siRNA) to knockdown the expression of total p63 (siGENOME SMARTPool, L-003330-00-0005, Dharmacon). The transfection was performed using Lipofectamine 2000 (11668-019, Invitrogen). Briefly, cells were seeded in 6-wells plates. Then, 0.05 nmol of siRNA diluted in 300μL of optiMEM (31985070, Life Technologies) was mixed with 4 μL of Lipofectamine 2000 diluted in 294 μL of optiMEM; the mixture was added into each well, resulting in a final volume of 600 μL. The medium was replaced with fresh medium after 6 h, and cells were collected after a total of 48 h to check the efficiency of silencing by Real Time PCR.

Gene silencing in LX-2 cells
LX-2 cells were transfected with specific small-interference RNA (siRNA) to knockdown the expression of total p63 (siGENOME SMARTPool, L-003330-00-0005, Dharmacon), ACC1 (siGENOME SMARTPool, L-004551-00-0005, Dharmacon) or HER2 (siGENOME SMARTPool, L-003126-00-0005, Dharmacon). Control group was administered with a non-targeting siRNA (siGENOME Non-Targeting siRNA Pool, D-001206-13-05, Dharmacon). The transfection was performed using Lipofectamine 2000 (11668-019, Invitrogen). Briefly, cells were seeded in 6-wells plates. Then, 0.05 nmol of each siRNA diluted in 300μL of optiMEM (31985070, Life Technologies) was mixed with 6 μL of Lipofectamine 2000 diluted in 294 μL of optiMEM; the mixture was added into each well, resulting in a final volume of 600 μL. The medium was replaced with fresh medium after 6 h, and cells were collected after a total of 48 h to check the efficiency of silencing by Real Time PCR.

Gene overexpression *in vitro*
For plasmid transfection in human LX-2 cells, we used a DNA plasmid containing the sequence necessary to increase the expression of pTAp63 (27008, Addgene), ΔNp63 (26979, Addgene),[59] HER2 (16257, Addgene)[60] and an empty plasmid as control. 6 μL of Lipofectamine 2000 diluted in 250 μL of optiMEM were mixed with 1 ng of plasmid DNA diluted in 250 μL of optiMEM. Next, 500 μL of this mixture was added into each well and incubated for 6 h. The medium was replaced with fresh medium, then cells were collected after a total of 24 h to check the efficiency of overexpression by Real Time PCR.

Metabolic flux assays
Mitochondrial respiration and glycolytic flux were evaluated by monitoring the oxygen consumption rate (OCR) and the extracellular acidification rate (ECAR), respectively, by high-resolution respirometry with the Seahorse Bioscience XFp Extracellular Flux Analyzer (Agilent Technologies). 2.0 x 10⁴ cells were seeded per well in a XFp cell culture microplate (103022-100, Seahorse Bioscience, Agilent Technologies). Previous to the assay, medium was removed, and replaced with pre-warmed assay medium, composed of Seahorse XF DMEM medium (103575-100 Seahorse Bioscience, Agilent Technologies) containing 1 mM sodium pyruvate, 2 mM L-glutamine and 10 mM glucose, and cultured at 37°C in room air. After equilibration in assay medium for 1 h, five basal measurements of OCR and ECAR were performed. Next, we sequentially added into cells wells the modulators of respiration oligomycin (Oligo, 1.5 μM), carbonyl cyanide-4 (trifluoromethoxy) phenylhydrazone (FCCP, 1 μM) and rotenone/antimycin (Rot/AA, 0.5 μM) to evaluate the mitochondrial function (Cell Mito Stress Test Kit, 103010-100, Seahorse Bioscience, Agilent Technologies); or Rot/AA followed by 2-Deoxyglucose (2-DG, 50mM) to evaluate the glycolytic function (Glycolytic Rate Assay Kit, 103346-100, Seahorse Bioscience, Agilent Technologies). The following key parameters of mitochondrial function were calculated according to the manufacturer's user guide: basal respiration, ATP-linked respiration, proton leak, maximal respiration, spare capacity and non-mitochondrial oxygen consumption (Cell Mito Stress Test Kit); basal glycolysis and compensatory glycolysis (Glycolytic Rate Assay Kit). All

results were normalized to protein content. Data of OCR during basal metabolism of Cell Mito Stress Test and ECAR during basal metabolism of Glycolytic Rate Assay were used in the graphs depicting the quiescent or energetic state of HSCs under different conditions.

TGFβ1 treatment
LX-2 cells transfected with sip63 or siCTL were incubated with medium supplemented with recombinant human TGFβ1 (100-21, PreproTech) at a concentration of 8 ng/mL or vehicle for 24 h.[44]

Firsocostat administration
Pharmacological inhibition of ACC was carried out by using Firsocostat, an allosteric ACC1/ACC2 inhibitor, also known as GS-0976 (HY-16901, MedChemExpress).[18] Firsocostat was administered in LX-2 cells at a concentration of 0.5 μM.[14]

CP724714 administration
Pharmacological inhibition of HER2/ErB2 was carried out by using a potent and selective inhibitor, also known as CP724714 (PZ-0335, Sigma-Aldrich). CP724714 was administered in LX-2 cells at a concentration of 50 nM (IC_{50}).

Autophagic flux
Autophagic flux was determined by analyzing LC3-II turnover by preventing lysosomal degradation, using 60 μM chloroquine (CQ) (H0915, Sigma-Aldrich) for the last 6 h of the experiments.[63] LC3-flux was calculated by subtracting the densitometry value of normalized LC3-II in the sample treated with CQ, by the value in the control sample (vehicle-treated). LC3-II flux was expressed relative to their respective controls.

ACC activity assay
Enzymatic activity of ACC was determined in LX-2 extracts by measuring Malonyl-CoA levels with the Mouse Malonyl coenzyme A ELISA Kit (MBS705127, MyBioSource) according to manufacturer's instructions. Briefly, 3×10^5 LX-2 cells were homogenized in 50 μL of PBS, and then the protein extract was used in each well for the sequential incubation steps in the provided 96-well plate. Absorbance was read at 450 nm and the amount malonyl-CoA calculated against the standard curve concentration, normalizing the results to protein content.

Cell proliferation
The evaluation of cell viability *in vitro* was performed with a (3(4,5-dimethylthiazol-2-yl)-2,5-diphenyltetrazolium bromide) (MTT) test (M2003, MERCK). First, LX-2 cells were seeded in a 96-well plate. Next, LX-2 cells were transfected with either pTAp63 or sip63. After 24 h, LX-2 downregulating p63 were exposed to TGFβ1 for 24 h. Finally, MTT and the solubilization of formazan were added, and the cell viability in each well was measured in terms of optical density at a wavelength of 570 nm.

In vitro luciferase assay in cells
For luciferase assays, LX-2 cells were transfected in 24-well plates containing Lipofectamine 2000, 1 ng of TAp63 and control pcDNA overexpression vectors, 1 μg of each luciferase reporter plasmids p-luciferase, pHER2-luciferase and pACC1-luciferase for 24 h. Luciferase was measured in a Mithras LB 940 apparatus (Berthold Technologies, Bad Wildbad, Germany).

Real-time PCR
RNA was extracted using Trizol reagent (15596018, Invitrogen) according to the manufacturer's instructions. 100 ng of total RNA were used for each RT reaction, and cDNA synthesis was performed using the M-MLV Reverse Transcriptase (28025013, ThermoFisher) and random primers. For real-time PCR, we used a QuantStudio 5 Real-Time PCR Instrument (Applied Biosystems) following the manufacturer's instructions and SYBR green PrecisionPLUS reagent (PPLUS-LR, PrimerDesign). The PCR cycling conditions included an initial denaturation at 95°C for 3 min followed by 40 cycles at 95°C for 5 s and 60°C for 32 s. The oligonucleotide specific primers are shown in Table S4. All reactions were performed in duplicate. Expression levels were normalized to HPRT for each sample and expressed in relation (%) to the control group.

Western blot
Western blots were performed as previously described.[9] Briefly, total protein lysates from liver (20 μg) or cells (5 μg) were subjected to SDS-PAGE, electrotransferred onto polyvinylidene difluoride membranes and probed with the antibodies indicated in the key resources table. For protein detection, horseradish peroxidase-conjugated secondary antibodies and chemiluminescence (Amersham Biosciences) were used. Membranes were exposed to radiograph film (Super RX Fuji Medical X--ray Film, Fujifilm) and developed with developer and fixing liquids (AGFA) under appropriate dark room conditions. Protein expression was quantified by densitometric analysis with ImageJ 1.52p software. Protein levels were normalized to GAPDH for each sample and expressed in relation to the control group. Uncropped blots accompanied by the location of molecular weight markers are shown in Appendix Figure 1.

QUANTIFICATION AND STATISTICAL ANALYSIS

Data are expressed as mean ± standard error mean (SEM). Statistical significance was determined by two-tail Student's *t* test when two groups were compared or ANOVA and post-hoc Bonferroni test when more than two groups were compared. To study the correlation between gene expression and different parameters, Spearman's correlation coefficients (r) were used. $p < 0.05$ was considered significant for all the analysis. Details for each analysis including test, p value, and number analyzed can be found in the figure legends or figures themselves. Analyses were performed with the Prism Software Version 9.5.1 (GraphPad).